hiPSC-derived Neural Stem/Progenitor Cells in Chronic Cervical Spinal Cord Injury

Samuel E Nutt

A dissertation
submitted in partial fulfillment of the
requirements for the degree of

Doctor of Philosophy

University of Washington
2012

Reading Committee:
Philip Horner (Chair)
Steve Perlmutter
Thomas Reh

Program Authorized to Offer Degree:
Neurobiology and Behavior

University of Washington

Abstract

hiPSC-derived Neural Stem/Progenitor Cells in Chronic Cervical Spinal Cord Injury

Samuel E Nutt

Chair of Supervisory Committee
Associate Professor Philip J Horner
Department of Neurological Surgery

Human induced pluripotent stem cells (hiPSCs) have the potential to provide plentiful autologous cells for clinical translation to spinal cord injury, but substantial hurdles remain. The necessary conditions for effective cell replacement and plasticity to occur in a safe manner are yet to be determined. This work evaluated the use of hiPSCs at three different differentiation states as potential therapeutic agents in chronic cervical spinal cord injury, a condition for which current treatment modalities are mostly ineffective. While driving hiPSCs to a fully differentiated state (i.e. astrocytes), with specific regional, morphological and phenotypic features, was feasible *in vitro*, hiPSC-derived astrocytes did not prove to be an effectively transplantable resource. Multipotent caudalized hiPSC-derived neural progenitor cells engrafted well into the hostile lesion environment and differentiated into multiple neural and glial cell types *in vivo* that translated into only modest functional recovery. Finally, transplantation of hiPSC-derived neural stem cells showed that broad differentiation potential brings a concomitant risk of overgrowth. Finding a balance between competency and unchecked proliferation will be key to effectively and safely realizing the potential of hiPSCs in spinal cord injury. Additionally, there is a need for solid preclinical foundation and demonstration of safety (both biological and procedural) before clinical trials can be attempted. Despite these caveats, hiPSC-derived neural cells still show promise as a means of inducing cellular plasticity in a vastly underserved population of patients suffering from chronic cervical SCI.

TABLE OF CONTENTS

List of Figures

Dedication

This dissertation is dedicated to my family.

Chapter I: INTRODUCTION

In mammalian embryogenesis, cell differentiation is tightly regulated and occurs in a strict temporal order. As cells divide and specialize through development, their options for final phenotype become progressively more limited until arriving at their ultimate fate. However, since differentiation is governed by epigenetic rather than genetic events, it is in theory a reversible process. In the last decade, the discovery that a combination of four transcription factors is sufficient to reprogram an adult human somatic cell to a pluripotent stage (Takahashi, Tanabe et al. 2007; Yu, Vodyanik et al. 2007) has opened a multitude of possibilities for personalizing medicine and modeling diseases in a dish. Human induced pluripotent stem cells (hiPSCs) meet the criteria for defining human embryonic stem cells (hESCs), i.e. prolonged undifferentiated proliferation and stable developmental potential to form derivatives of all three embryonic germ layers (Thomson and Marshall 1998). hiPSCs are grown under embryonic stem cell conditions and can be differentiated into many cell types of an adult affected by a particular condition while maintaining their underlying genetic background (Maherali, Sridharan et al. 2007; Park, Arora et al. 2008; Brennand, Simone et al. 2011). As such, hiPSCs can be used for studying development and function of somatic cells, for transplantation therapies, and for testing new pharmacologic treatments. And in contrast to hESCs, hiPSCs do not require embryonic material, thus obviating practical and ethical concerns of working with human embryonic tissue. Another putative advantage of hiPSCs over hESCs is the potential for autologous cell transplantation, as hiPSCs can be derived from a patient's own somatic cells, thus avoiding immune system suppression.

Once patient fibroblasts are reprogrammed into hiPSCs, they can subsequently be differentiated into neurons and glia for use as potential cell-based therapies for a wide range of central nervous system (CNS) disorders. Pluripotent stem cells also offer an opportunity to regionally specify cells via patterning cues, something that cannot be accomplished with mature neural stem cells (NSCs). In the last few years, researchers have published investigations of hiPSC-derived neural cells in a wide variety of neurodegenerative and neurodevelopmental disorders, including amyotrophic lateral sclerosis (ALS) (Dimos, Rodolfa et al. 2008), Parkinson's disease (Park, Arora et al. 2008; Soldner, Hockemeyer et al. 2009; Rhee, Ko et al. 2011), spinal muscular atrophy (Ebert, Yu et al. 2009), stroke (Oki, Tatarishvili et al. 2012), Alzheimer's disease (Israel, Yuan et al. 2012) and schizophrenia (Brennand, Simone et al. 2011). The ability of hiPSCs to differentiate into clinically relevant neural cell types makes them an accessible autologous source for cell replacement, and a resource for detailed investigation of pathogenetic mechanisms.

The appropriate cell population and conditions for transplants will depend on the disease being studied, and may even vary from patient to patient. The variables to consider include cell number, cell type, degree of differentiation (e.g. stem cell, progenitor cell, fully differentiated neuron), location and timing of transplant, and co-therapies such as rehabilitation or pharmacologic intervention. Degree of differentiation is particularly important, as cell survival is typically poor after transplantation of fully differentiated neural cells, especially neurons and oligodendrocytes (Rhee, Ko et al. 2011; Yuan, Martin et al. 2011). Relatively immature cells are likely to show more robust survival after transplant, particularly in the hostile environment of disease or injury. Less differentiated cells, however, may carry a risk of overgrowth, tumor formation, and the concomitant deleterious effects. Cells at any stage can be contaminated with

undifferentiated cells, posing the potential to generate teratomas. Thus, rational selection of cells to be transplanted is paramount.

There is a limited amount of data on the utility of hiPSC-derived cells in spinal cord injury (SCI). Traumatic SCI results in substantial loss of neuronal and glial elements of the spinal cord, cavitation and glial scarring. SCIs involve the primary physical injury followed by a secondary injury phase defined by pathophysiological processes such as inflammation, ischemia, axon demyelination, and glial scarring (astrogliosis) (Tator and Fehlings 1991). Stem cells of various stages of differentiation are of particular value in SCI and regenerative medicine in general. Cell transplantation strategies are typically designed to enhance endogenous axon regeneration, functionally replace dead cells and/or create a microenvironment conducive to regeneration or remyelination. Early CNS regeneration research focused on bridging the lesion with a microenvironment conducive to axon growth via transplants of peripheral nerve (David and Aguayo 1981) or embryonic CNS tissue (Nornes, Bjorklund et al. 1983). More recently, transplanted neural stem cells derived from various rodent tissues have induced moderate axonal sprouting (Pfeifer, Vroemen et al. 2004; Hofstetter, Holmstrom et al. 2005; Karimi-Abdolrezaee, Eftekharpour et al. 2010). Neuronal cell replacement strategies, however, are likely of limited clinical application in SCI due to the length of tracts involved and their close physical association with pain fibers, which could participate in neuropathic pain syndromes or spasticity. Thus, replacement strategies are perhaps better targeted toward recreating the intact glial environment, modifying the lesion, and sparing tissue. Indeed, transplantation of astrocytes into the CNS has proven beneficial with respect to regeneration and neuroprotection (Smith, Miller et al. 1987; Hofstetter, Schwarz et al. 2002; Lepore, Rauck et al. 2008; Kumagai, Okada et al. 2009;

Tsuji, Miura et al. 2010). Immature astrocytes are especially effective at supporting neurite outgrowth and suppressing formation of the glial scar, a key physical and chemical barrier to regeneration (Smith, Rutishauser et al. 1990; Smith and Miller 1991; Filous, Miller et al. 2010). In addition to targeting the replacement and repair of neurons and glia, neural stem/progenitor cell transplantation can be used to induce immunomodulation, angiogenesis and trophic support of endogenous cells and circuits (Teng, Lavik et al. 2002; Teng, Liao et al. 2006; Tebar, Geranton et al. 2008).

Two studies to date have reported the use of hiPSC-derived cells for spinal cord injury, both in the thoracic region with transplantation occurring at sub-acute time points (7-9 days post-injury) (Nori, Okada et al. 2011; Fujimoto, Abematsu et al. 2012). While they both demonstrated mild efficacy in effecting locomotor recovery, the most common region affected in SCI is the cervical region (approximately 50-60% of human SCI (National Spinal Cord Injury Statistical Center 2011)). Further, among those with cervical SCI, regaining function in the hands and arms is the most critical determinant of quality of life (Anderson 2004). This likely correlates to the fact that even partial or mild arm, hand or shoulder function can have an enormous impact on independence, and independence enhances quality of life (Mulcahey, Smith et al. 1994; Waters, Sie et al. 1996; Franceschini, Di Clemente et al. 2003; Wuolle, Bryden et al. 2003).

While scientific understanding of CNS regeneration has advanced substantially in the last 25 years, many unknowns remain with regard to successful regeneration that induces functional recovery, especially in the chronic SCI state (Blight 2002; Hulsebosch 2002; Kwon, Oxland et al. 2002; Filbin 2003; Houle and Tessler 2003). The gaps in current knowledge make chronic transplant models of substantial scientific value, in addition to potentially benefitting the 1.275

million patients currently living with chronic spinal cord injury (CDRF 2009). Thus, the use of a chronic cervical SCI model would be clinically relevant to a large number of patients.

On a pathophysiologic level, treating chronic SCI presents additional challenges to those faced in acute SCI, a fact borne out by observation that most therapies that show benefit early after injury prove to be ineffective when administered at chronic time points (Houle and Tessler 2003). Prohibitive mechanisms include: glial scars and inhibitory extracellular matrix molecules that are well-established around the lesion (Busch and Silver 2007), neuronal atrophy and downregulation of regeneration-associated genes (Kwon, Liu et al. 2002), and axonal degeneration in both anterograde and retrograde directions (Pallini, Fernandez et al. 1988; Houle and Tessler 2003). Collectively, these processes create an environment especially refractory to regeneration and plasticity. Additionally, many of the therapies that show efficacy in acute and subacute settings do so through mechanisms that are neuroprotective or augment spontaneous recovery, which has ceased by chronic time points (Jacob, Hacker et al. 2001; Geller and Fawcett 2002).

All treatments for spinal cord injury would optimally be accompanied by safety assessments that monitor measures including pain syndromes and maintenance of function in any spared tissue. The latter is of particular importance in the cervical region, where circuitry for many critical functions such as respiration resides and thus exacerbation of damage must be avoided. Cell-based therapies for SCI have many concerns specific to cellular transplantation, including biological contamination, undesired migration, overgrowth, and tumor formation. Cells derived from stem cells, especially pluripotent stem cells, carry the risk of contamination with undifferentiated cells that are particularly prone to overgrowth and tumors (Bjorklund, Sanchez-

Pernaute et al. 2002; Erdo, Buhrle et al. 2003; Roy, Cleren et al. 2006; Hedlund, Pruszak et al. 2007; Pruszak, Sonntag et al. 2007; Wernig, Zhao et al. 2008; Miura, Okada et al. 2009; Tsuji, Miura et al. 2010; Doi, Morizane et al. 2012). Even benign growths in the cervical spinal cord can have severe consequences, for the reasons described above. Thus long-term followup and observation in preclinical models is necessary to ensure freedom from adverse events.

This work focuses on the development and characterization of region-specific hiPSC-derived neural stem cells (hiPSC-NSCs), neural progenitor cells (hiPSC-NPCs), and glia, and their ability to effect plasticity in the chronic contused spinal cord. My initial hypothesis was that hiPSCs could be induced to form immature astrocytes through multiple defined biochemical pathways, and that these glia would support intraspinal plasticity and behavioral recovery in a novel chronic cervical contusion model of SCI. While hiPSCs are capable of forming hindbrain/spinal cord-specific astrocyte subtypes with important phenotypic differences *in vitro* and *in vivo*, they do not survive well in the naive adult spinal cord and therefore appear ill-suited to effecting recovery after injury. Less differentiated neural precursors (i.e. hiPSC-NSCs and hiPSC-NPCs), however, do successfully integrate into the chronic injury environment and generate both neuronal and glial phenotypes (including astrocytes), but in a manner that induces only modest recovery. Still, even incremental improvement in function can have a profound impact on the level of independence and quality of life of cervical SCI patients, suggesting that even the small benefit reported here could be of value if translated to humans. With these results, however, comes the caveat that rigorous safety measures must be in place when considering hiPSCs and their progeny for clinical trials, as tumorigenesis is possible with certain immature cell populations, particularly hiPSC-NSCs.

CHAPTER II: Induction of human iPSC-derived astrocytes with bone morphogenetic protein-4 or glycoprotein 130 agonists

Summary

In the injured CNS, transplanted immature astrocytes (either primary or derived from glial precursors) are more conducive to regeneration, neuroprotection and glial scar suppression than mature or reactive ones. Glial precursors treated with BMP-4 or CNTF to induce astrocyte formation have differential effects on SCI recovery, allodynia, and hyperalgesia. hiPSCs provide an ideal technology for generation of immature astrocytes via different pathways, though the temporal requirement may be significant. I tested whether BMP-4, CNTF and CT-1 would have different effects on properties of hiPSC-NSCs, in terms of astrocyte differentiation *in vitro* and behavior *in vivo*. Region-specific hiPSCs-NSCs required substantial long term *in vitro* expansion before becoming capable of astrocyte generation, but astrogliogenesis was achieved earlier than previous reports. BMP4 and gp130 agonists both induced GFAP, but had distinct effects on morphology, survival and expression of mature astrocyte markers such as GLAST. After transplantation into the naive spinal cord, BMP4-treated cells showed better survival than CNTF- or CT-1-treated cells, and retained their astrocyte and posterior identity.

Introduction

Human induced pluripotent stem cells (hiPSCs) have many potential scientific applications, including understanding of early human development and use as a transplantable resource for various injury and disease states. Controlled differentiation of hiPSCs along specific lineages

will be a vital component of these applications. Many successful attempts have been made to induce hiPSCs and/or human embryonic stem cells (hESCs) to generate cells of a neural lineage, including neural stem cells (NSCs) (Zhang, Wernig et al. 2001; Chambers, Fasano et al. 2009; Nori, Okada et al. 2011; Yuan, Martin et al. 2011), neurons (Chambers, Fasano et al. 2009; Hu and Zhang 2009; Brennand, Simone et al. 2011; Rhee, Ko et al. 2011) and oligodendrocytes (Hu, Du et al. 2009; Hu, Du et al. 2009). Only one study to date, however, has demonstrated the capacity of hiPSCs to form astrocytes (Krencik, Weick et al. 2011), defined solely as a GFAP-positive cell. No study to date has detected the expression of mature astrocyte markers in hiPSC-derived cells, or demonstrated their ability to integrate into the adult CNS.

Insight into the development of human astrocytes is relatively scarce. Astrocyte specification is largely believed to happen in a uniform manner and perhaps "by default" (Doetsch 2003; Ross, Greenberg et al. 2003). Astrocyte genesis occurs after neurogenesis, as astroglial progenitors differentiate to immature astrocytes, which are critical for functional synapse formation (Ullian, Sapperstein et al. 2001; Johnson, Weick et al. 2007). In the adult CNS, astrocytes continue to play an essential role in synapse homeostasis, as well as regulating microvasculature (Iadecola and Nedergaard 2007) and supplying energy metabolites (Rouach, Koulakoff et al. 2008). Disruption of normal astrocyte function is implicated in numerous human diseases, including ALS (Nagai, Re et al. 2007), Huntington's disease (Bradford, Shin et al. 2009), Alexander disease (Brenner, Johnson et al. 2001), epilepsy (Oberheim, Tian et al. 2008), and astrocytomas. Thus, insight into the generation and maintenance of astrocytes has broad potential clinical benefit.

Despite the relative paucity of characterization, the functional and molecular diversity of astroglia has become better appreciated in recent years (Halassa, Fellin et al. 2007; Sofroniew 2009; Matyash and Kettenmann 2010; Yang, Vidensky et al. 2011). This heterogeneity manifests itself in many respects, including morphology, growth rates (Emsley and Macklis 2006), electrophysiological properties (Guatteo, Stanness et al. 1996), glutamate uptake (Drejer, Larsson et al. 1982; Israel, Schipke et al. 2003), gap junction coupling (Lee, Kim et al. 1994; Blomstrand, Aberg et al. 1999), and gene expression profiles (Bachoo, Kim et al. 2004; Yeh, Lee da et al. 2009). These differences imply the existence of multiple subtypes of astrocytes, whose functions may depend on environmental, temporal and regional factors (Hewett 2009; Matyash and Kettenmann 2010; Zhang and Barres 2010; Haas, Neuhuber et al. 2012; Molofsky, Krenick et al. 2012).

There are numerous known positive regulators of astrocyte differentiation, including bone morphogenetic proteins (BMPs) (Brimble, Zeng et al. 2004; Zhang and Li 2005), ciliary neurotrophic factor (CNTF) (Johe, Hazel et al. 1996), and cardiotrophin-1 (CT-1) (Ochiai, Yanagisawa et al. 2001). BMPs exert intracellular effects through activation of SMAD proteins, while CNTF and CT-1 are members of the interleukin-6 (IL-6) family that bind to glycoprotein 130 (gp130) receptor complexes that in turn activate the JAK/STAT pathway. The fact that these signals effect differentiation by different intracellular pathways, combined with the functional variety described above, renders the idea that astrocyte differentiation occurs “by default” (i.e. simply in the absence of neurogenic signals) less plausible. hiPSCs provide a unique opportunity to apply different astrogenic cues to human pluripotent cells and study the generation of various astrocyte subtypes.

Transplanting astrocytes into the CNS can be conducive to regeneration and neuroprotection (Smith, Miller et al. 1987; Hofstetter, Schwarz et al. 2002; Lepore, Rauck et al. 2008; Kumagai, Okada et al. 2009; Tsuji, Miura et al. 2010), though their benefit can depend on the differentiation pathway through which they are formed (Davies, Proschel et al. 2008; Davies, Shih et al. 2011; Haas, Neuhuber et al. 2012). Immature astrocytes in particular are more effective at supporting neurite outgrowth and suppressing glial scar formation (Smith, Rutishauser et al. 1990; Smith and Miller 1991; Filous, Miller et al. 2010). This study examined the ability of multiple cytokines, alone and in combination, to induce GFAP and the glutamate aspartate transporter GLAST, a mature astrocyte marker, in hiPSCs. I also transplanted these hiPSC-derived astrocytes into the adult spinal cord to test their ability to survive and retain phenotypes in the CNS.

Materials and Methods

Cell Culture

All hiPSC and hESC cells were grown as colonies in TeSR2 on Matrigel.

Dual SMAD inhibition

Colonies were treated with Accutase at room temperature until rendered to single cells. Cells were then plated on Matrigel in DMEM:F12 + KSR + ROCK inhibitor (Tocris Y-27362 dihydrocholoride) until >90% confluent (~2-3 days). Once cells were confluent (considered Day 1 of differentiation), the medium was changed to KSR + Noggin (500 ng/ml) + 10μM TGFβ-inhibitor (Tocris SB431542). On Day 5 of differentiation, the TGFβ-inhibitor was withdrawn and

increasing amounts of N2 (25%, 50%, 75%) were added to the KSR medium every other day while maintaining 500 ng/ml Noggin.

EB neuralization

On Day 0 of differentiation, colonies were separated from their substrate with 1.925 units/ml dispase and cultured in suspension in T75 flasks in TeSR2 and 10μM Y-27632. On Day 4, embryoid bodies (EBs) are switched to neural differentiation medium (NDM: DMEM/F12 containing N2, MEM non-essential amino acids, 2 μg/ml heparin) and 20 ng/ml FGF. On Day 7, EBs are plated on Matrigel in NDM + FGF. On Day 10, 0.1 μM retinoic acid (RA) is added to the medium. On Day 15, colonies possessing neural tube-like rosettes are mechanically detached and cultured in NBEF (NDM + B27 + 20 ng/ml EGF + 20 ng/ml FGF). Cells are cultured either as a monolayer on Matrigel, or in suspension as neurospheres in T75 flasks.

Treatment w/ BMP4, CNTF, etc.

For differentiation into astrocytes, hiPSC-NSCs were plated onto Matrigel-coated glass coverslips. Base differentiation medium for all conditions was NDM (described above) containing 1 μM cAMP. CNTF, CT-1 and BMP4 were all used at 10 ng/ml, unless otherwise stated. Cells were cultured in their differentiation medium for 2 weeks.

Immunofluorescence (Cells)

After fixation with 4% paraformaldehyde for 20 minutes, the cells were incubated with 10% donkey serum for 1 hour, then incubated in primary antibodies overnight at 4ºC. After a PBS wash and incubation with secondary antibodies at RT for 2 hours, nuclei were counterstained with 4’,6-diamidino-2-phenylindole (DAPI) and mounted.

Stereology

Stereology was conducted using a Zeiss Axioplan microscope and StereoInvestigator software (MBF Biosciences). Markers were quantified as percentages of DAPI-positive cells.

Animals and Surgeries

Adult female Long-Evans rats were used in this study. Animals received intraperitoneal injections of 80 mg/kg ketamine and 15 mg/kg xylazine. A laminectomy was performed at the C4 spinous process of the lamina. The animals were then placed in a spinal frame, and a pulled glass capillary (OD 70-100 μm) was placed on the lateral border of the gray matter and stereotactically lowered to a depth of 1.0 mm, targeting the gray-white border of the dorsolateral funiculus. Animals received two injections of 100,000 cells each (1.0 μl injected over 60 s), one rostral and one caudal to the injury site. Cells were treated with BMP4, CNTF, or CT-1, or maintained in NBEF, for two weeks prior to transplant (n=3 per group). Muscles were subsequently sutured in two layers and the skin closed. All animals received daily subcutaneous injections of cyclosporine (10 mg/kg, Sandimmune) from the day of transplant to the time of sacrifice, 10 days after transplant.

Tissue Processing

Animals were anesthetized and perfused transcardially with saline followed by 4% paraformaldehyde (PFA) in 0.1M phosphate buffer. Spinal columns were post-fixed overnight, cryoprotected with 30% sucrose, and then cut into five 1-mm coronal sections surrounding the lesion, embedded in OCT medium and flash frozen. 20 μm sections were cut on a Leica CM1850 cryostat in a one-in-six series and stored at -80ºC.

Immunofluorescence (Tissue)

Tissue was permeabilized with 0.4% Triton, then blocked with 5% donkey serum (DKS) and 0.4% Triton. Primary antibodies were applied to sections at 4˚C overnight. Slides were then rinsed 3 times in PBS, and incubated in the appropriate secondary antibody solution overnight at 4˚C. Sections were rinsed twice more with PBS, then incubated with DAPI before mounting.

Antibodies

The following antibodies were used: GLAST (Abcam, 1:100), hGFAP (StemCells, Inc., 1:1000), HoxB4 (Developmental Studies Hybridoma Bank, 1:100), HuNu (Millipore, 1:300), Sox1 (R&D Systems, 1:500), Sox9 (R&D Systems, 1:500), and TuJ1 (Covance, 1:1000).

Study Approval

All animal-related procedures were approved by the Institutional Animal Care and Use Committee of the University of Washington and were conducted in accordance with the guidelines of the NIH.

Results

Comparison of neuralization efficiency of pluripotent stem cells

Two methods for the induction of neuroepithelia were employed: (1) embryoid body (EB) formation followed by rosette induction, or (2) dual SMAD inhibition by application of Noggin and the TGFβ-inhibitor SB431542. Both methods successfully neuralized all hESC and hiPSC lines tested, though with highly variable efficiency (Fig. 1a-c). All cell lines neuralized via EB formation yielded a high proportion (>85%) of cells expressing the homeobox gene HoxB4, a hindbrain/spinal cord-specific marker indicating posterior identity (Bass and Baker 1997; Hu and Zhang 2009). In contrast, those exposed to dual SMAD inhibition exhibited low HoxB4

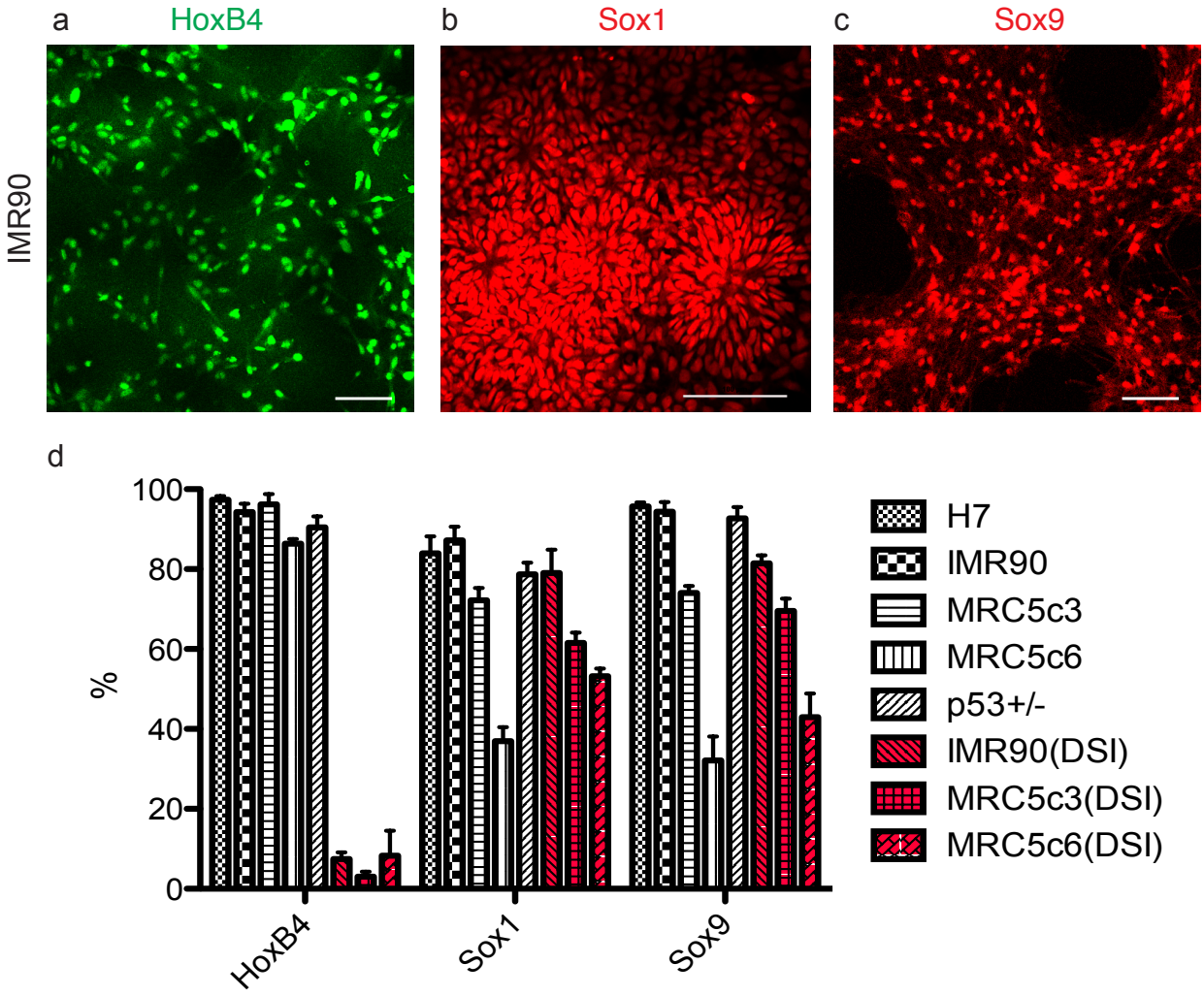

Figure 1 | Efficiency of neural differentiation and patterning of hESCs and hiPSCs. (**a-c**) hiPSCs acquire neural and region-specific markers after differentiation. IMR90 hiPSCs differentiated via the embryoid body method express the homeobox gene HoxB4 (**a**), the neuroepithelial marker Sox1 (**b**), and the neural stem cell marker Sox9 (**c**). (**d**) Percentage of cells positive for HoxB4, Sox1, and Sox9, for each cell line and induction method. DSI refers to cells differentiated via dual SMAD inhibition (red bars). Scale bars = 100 μm.

expression (<10%), presumably due to the absence of retinoic acid administration in this protocol (Fig. 1d).

Highest neuralization efficiency was achieved from hiPSCs derived from IMR90 fibroblasts or from fibroblasts obtained from a patient heterozygous for the tumor suppressor gene p53 (p53+/-). MRC5c6 hiPSCs were the least efficient in generating Sox1-positive and Sox9-positive cells, regardless of neuralization method. Generally, for a given cell line, neuralization efficiency as assessed by Sox1 or Sox9 was comparable when comparing EB and SMAD inhibition. As IMR90 hiPSCs yielded NSCs with the greatest efficiency, all subsequent experiments were performed with IMR90 hiPSC-NSCs.

Morphologic and phenotypic analysis of hiPSC-derived astrocytes

Prior to treatment, only 1.03% of hiPSC-NSCs were GFAP-positive. To induce astrocyte differentiation, cultures of IMR90 hiPSC-NSCs were treated with BMP4, CNTF, or CT-1 for two weeks. Upon exposure to these factors, hiPSC-NSCs did not express GFAP when administered immediately after neuralization (data not shown). However, when hiPSC-NSCs generated through the EB method were maintained in proliferation medium for several months, then exposed to BMP4, CNTF or CT-1, widespread GFAP expression could be seen (Fig. 2a).

After two weeks of treatment with the BMP4, CNTF or CT-1, groups differed with respect to survival, morphology and phenotype. BMP4-treated hiPSC-NSCs showed slightly poorer survival than undifferentiated hiPSC-NSCs or those treated with gp130 agonists. BMP4-treated hiPSC-NSCs displayed a multipolar morphology, with many broad, short processes expressing filamentous GFAP (Fig. 2a). CNTF- and CT-1 treated hiPSC-NSCs, however, adopted a bipolar or tripolar, radial glia-like morphology, with long thin processes that extended up to hundreds of

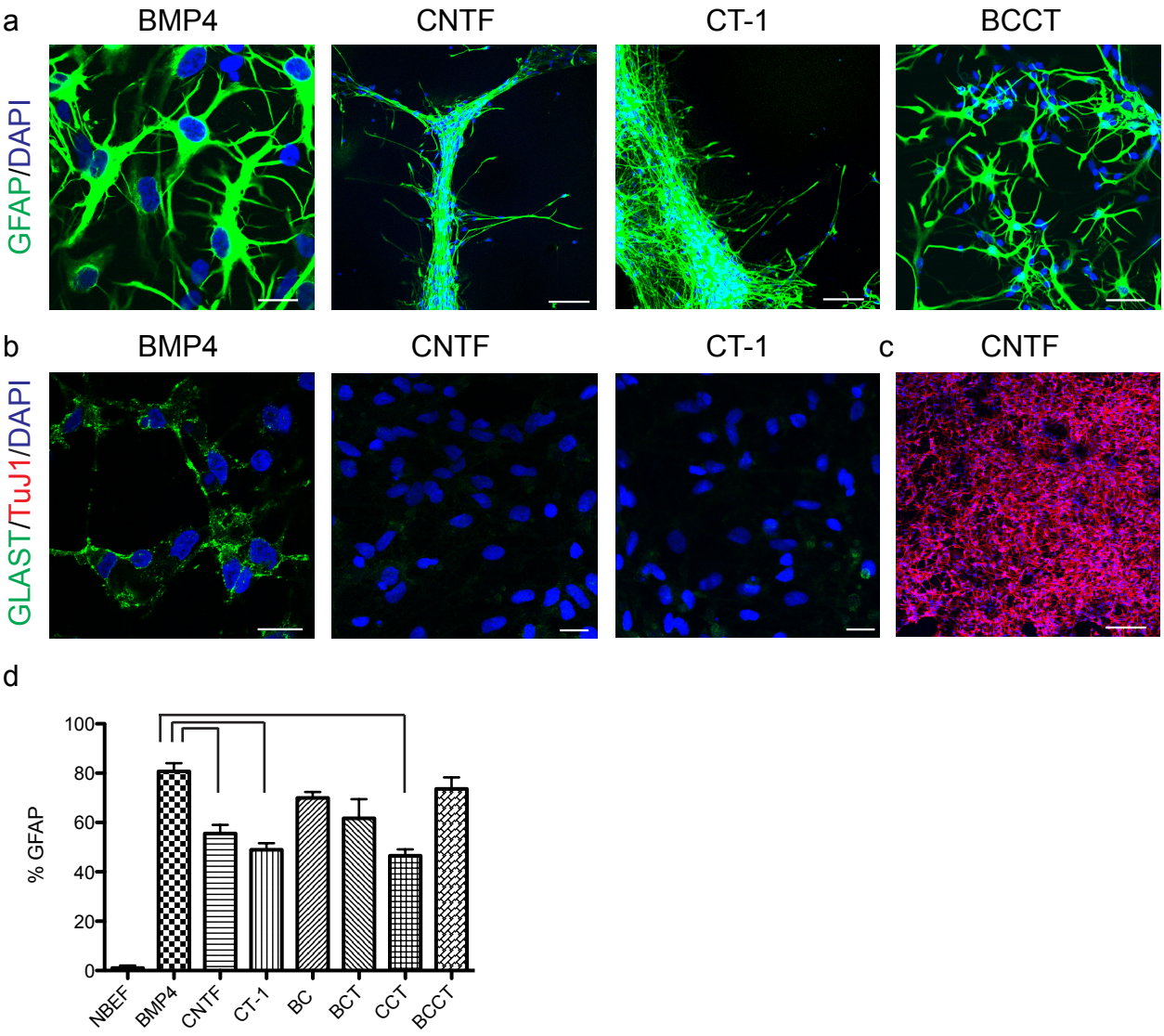

Figure 2 | Phenotypic analysis of IMR90 hiPSC-derived astrocytes.
(**a**) GFAP (green) in cells treated with various cytokines. (**b**) BMP-4 induced GLAST (green) expression, while CNTF and CT-1 did not. (**c**) CNTF-treated cells express TuJ1 (red) in addition to GFAP. (**d**) Comparison of efficiency in generating GFAP+ cells across treatments. All treatments resulted in significantly more GFAP than hiPSC-NSC proliferation medium (NBEF). BMP4 treatment generated more astrocytes than any treatments without BMP4 (CNTF, CT-1, CCT). Scale bars = 50 µm (**a**), 20 µm (**b**) or 200 µm (**c**). Error bars are SEM. Solid lines above bars in D = $p < 0.01$. BC = BMP4 + CNTF, BCT = BMP4 + CT-1, CCT = CNTF + CT-1, BCCT = BMP4 + CNTF + CT-1.

microns (Fig. 2a). Despite this morphology, CNTF/CT-1 treated cultures did not express the radial glia marker RC1 (data not shown). These cells tended to form networks with bundles of parallel cell processes connecting islands of cell nuclei.

BMP4-treated hiPSC-NSCs were the only cells to express the mature astrocyte marker GLAST (Fig. 2b). No CNTF or CT-1-treated cells were GLAST-positive, indicating a less mature phenotype. A proportion of cultures grown with CNTF contained cells positive for the pan-neuronal marker TuJ1 (Fig. 2c), while BMP4 and CT-1 treated cells did not.

80.7% of BMP4-treated cells expressed GFAP, while 55.6% of CNTF-treated cells and 48.93% of CT-1-treated cells were GFAP-positive. For quantification of GFAP, four additional differentiation media were attempted in order to assess potential synergistic influences on astrocyte generation: BMP4 + CNTF, BMP4 + CT-1, CNTF + CT-1, and BMP4 + CNTF + CT-1. All treatments, with single or multiple cytokines, resulted in significantly more GFAP than undifferentiated controls (Fig. 2d). Generally, treatments that included BMP4, irrespective of additional cytokines, had the same morphological and phenotypic results as BMP4 alone (Fig. 2a, d). BMP4 treatment resulted in significantly more astrocytes than CNTF, CT-1 or CNTF and CT-1 together.

Survival and retention of phenotype in vivo

I then tested the ability of these cells to survive *in vivo* by transplanting them into the dorsolateral funiculus of the intact adult rat spinal cord. Ten days after transplantation, survival across groups was poor, particularly in the CNTF and CT-1 groups. Transplantation of undifferentiated hiPSC-NSCs resulted in the best survival, with many hGFAP-positive cells detected in both the gray and white matter of the spinal cord. BMP4-treated cells also survived

well and retained astrocyte identity (Fig. 3a) as well as region specificity, as determined by HoxB4 reactivity (Fig. 3b). Even though CNTF-treated cells were infrequently detected *in vivo*, their phenotype profile was similar to that seen *in vitro*, with both hGFAP+ astrocytes (Fig. 3c) and TuJ1+ neurons (Fig. 3d) observed.

Discussion

Induction of neuroepithelia could be accomplished effectively through multiple methods applied to pluripotent stem cells, but generation of mature astrocytes required *in vitro* expansion and was best achieved through administration of BMP4. The yields of EB induction and dual SMAD inhibition were similar for a given line, but neuralization efficiency varied somewhat across lines. Long-term (3 months) *in vitro* expansion of hiPSC-NSCs was required before generation of astrocytes was possible. BMP4 treatment of hiPSC-NSCs resulted in stellate GFAP+ cells that also expressed the mature astrocyte marker GLAST, while treatment with gp130 agonists resulted in fewer GFAP+ cells that had a more immature morphology and lacked expression of mature astrocyte markers. Transplant of hiPSC-derived astrocytes into the adult rat spinal cord resulted in better survival with the BMP4-treated cells, which retained their astrocyte identity *in vivo*.

The two neuralization methods used here employ substantially different techniques that have important implications for the phenotype of the hiPSC-NSCs generated. Most publications involving the neuralization of hiPSCs employ some method of EB induction, though specifics with regard to timing and reagents vary highly. An advantage of EB induction is conferring posterior identity, which may make cells better suited for transplantation into the spinal cord.

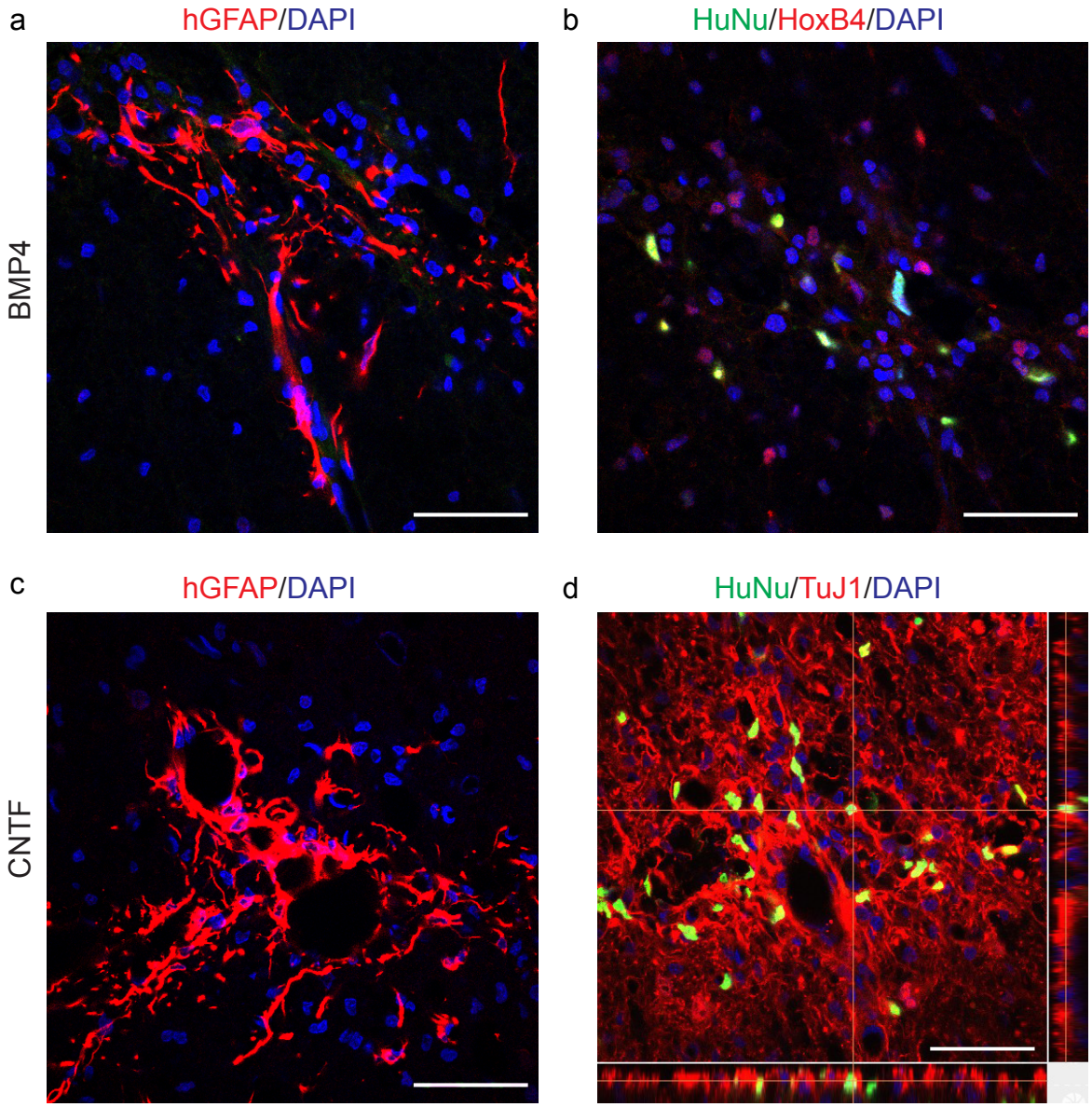

Figure 3 | hiPSC-derived astrocytes in the intact rat spinal cord.
a, BMP4-generated astrocytes in the white matter of the spinal cord. **b**, Colocalization of HuNu and HoxB4 shows that BMP4-treated cells retain their posterior identity in the spinal cord. **c-d**, CNTF-treated hiPSC-NSCs generated both astrocytes (**c**) and TuJ1+ neurons (**d**) *in vivo*. Scale bars = 50 µm.

Future work should test whether the region specificity is in fact advantageous with regard to cell survival, phenotype, and behavior function in an injury model. It is possible that posterior identity could be achieved through dual SMAD inhibition simply via incorporation of retinoic acid, as previous studies with hESCs and hiPSCs have shown the requirement of RA for HoxB4 acquisition (Hu and Zhang 2009; Krencik, Weick et al. 2011). The dual SMAD inhibition method has the advantages of homogeneity of cultures and relative rapidity of induction. Yields were similar to the EB method, but this is due in part to the inclusion in the EB method of selection of rosette-containing colonies, which functions as a purification step. As a percentage of all hiPSCs at the beginning of induction, yields would technically be much higher with dual SMAD inhibition.

There is a burgeoning interest in the heterogeneity of astrocytes due to mounting evidence that they are not simply stroma-like cells that primarily provide structural and homeostatic support for neurons. Enhanced understanding of astrocyte function has led to a concomitant view that astrocytes are not homogeneous, an idea that has important implications for the development of the therapeutic potential of astrocytes in CNS injuries, itself a relatively recent revelation. Attempts to induce astrocyte phenotypes immediately after neuralization proved unsuccessful with both neuralization methods. Acquisition of GFAP required prolonged *in vitro* expansion of hiPSC-NSCs, consistent with developmental principles (Rowitch and Kriegstein 2010). Krencik et al showed that GFAP acquisition happens spontaneously (i.e. without BMP4, CNTF or other astrogenic cues) in hiPSCs, with 65% and 90% of neural progenitors expressing GFAP after 120 and 180 days, respectively, of *in vitro* expansion. Here, I was able to achieve up to 80% GFAP reactivity after only 90 days of *in vitro* expansion. Still, this is substantially longer than rodent

pluripotent cells, which take on the order of days or weeks to generate GFAP+ astrocytes. It is possible that this finding reflects the temporal differences in ontogeny among species, as rodent development occurs over a much shorter time course than human. Attempts at generating astrocytes from hiPSC-NSCs derived via dual SMAD inhibition after long-term expansion should be performed in future studies to see if the same principles apply.

BMP4 treatment of hiPSC-NSCs resulted in more morphologically and phenotypically mature astrocytes. There were significantly more GFAP+ cells with BMP4 than the gp130 agonists (alone or in combination). The shorter, more numerous processes as well as GLAST expression suggested a more definitive astrocyte phenotype. I also evaluated the effects of changing BMP-4 concentrations (up to 100 ng/ml) but this lead to increases in cell death without significant changes in morphology or phenotype among surviving cells. Experiments with *in vitro* assays to demonstrate glutamate buffering in these cells would be useful in demonstrating functionality of these transporters.

While treatment with CNTF or CT-1 (or both) appeared to confer GFAP-reactive cells, they were less convincing of astrocyte identity, as they did not express more mature astrocyte markers. They were also more radial glia-like in morphology, though they did not stain positively for the radial glia marker RC-1. CNTF also induced substantial TuJ1, consistent with its described neurogenic role (Emsley and Hagg 2003). Generally, combination of BMP4 with gp130 agonists resulted in cultures more similar to the BMP4 alone than C/CT/CCT in terms of percent GFAP reactivity and morphologies, suggesting that BMP4 exerts a greater influence over phenotype than CNTF or CT-1. Previous studies showed a synergistic effect on astrocyte differentiation between BMP4 and LIF (Nakashima, Yanagisawa et al. 1999; Nakashima, Yanagisawa et al.

1999; Yanagisawa, Nakashima et al. 2001; Weible and Chan-Ling 2007), another member of the IL-6 gp130 agonist family, yet no such result occurred with the factors tested here. Whether such signaling crosstalk would occur with a BMP4/LIF combination or simply does not exist in hiPSC-derived cells remains to be seen.

The morphological and phenotypic differences among groups closely parallel previous results with astrocytes generated from embryonic rat glial restricted precursors (GRPs) (Haas, Neuhuber et al. 2012). Haas et al showed that BMP4-derived astrocytes were more mature and had a stellate morphology, while CNTF-treated GRPs were GFAP+, but retained immature markers and elaborated long processes. Davies et al also treated GRPs of human fetal and embryonic rat origin with BMP4 and CNTF (Davies, Proschel et al. 2008; Davies, Shih et al. 2011). The morphologies reported by Davies differed markedly from those reported here and by Haas et al, but the general observation that BMP4 resulted in more mature cells than CNTF applied, at least to the rat GRPs. These observations with embryonic rat cells are consistent with my results with hiPSCs, suggesting conservation of certain principles of astrocyte genesis across species. Haas et al did not employ CT-1, but did treat GRPs with FBS, which resulted in the most mature and homogeneous astrocytes. In contrast, attempts to treat hiPSC-NSCs with FBS resulted in no GFAP expression and spindle-like fibroblast morphologies (data not shown).

Haas's GRP-derived astrocytes generated via BMP4/CNTF treatment retained considerable plasticity, such that when challenged with the complementary factor, FGF, or FBS, differentiated astrocytes would change or even reverse phenotypes. Whether similar plasticity occurs in hiPSC-derived astrocytes remains to be seen, but BMP4-treated astrocytes did retain their phenotype and regional specificity after transplant (see below). This is an important consideration given that

BMP-induced differentiation of mouse embryonic cells into astrocytes can be reversed by withdrawal of the protein (D'Alessandro and Wang 1994).

Transplant of populations of treated and untreated hiPSC-NSCs into the adult rat spinal cord resulted in variable survival. Undifferentiated hiPSC-NSCs showed the most robust survival, followed by BMP4-treated cells. CNTF and CT-1 treated cultures did not survive well *in vivo*. BMP4-treated hiPSC-NSCs retained both astrocyte and posterior identity, the latter of which suggests that early patterning has phenotypic effects that are maintained long term. Future studies in which caudalized hiPSC-NSCs are transplanted into the forebrain would be useful in determining if posterior identity is retained even in an anterior region of the CNS. With regard to hiPSC strategies for delivery of neurons, relatively less differentiated NSC/NPCs show more robust survival than mature neurons (Rhee, Ko et al. 2011; Yuan, Martin et al. 2011; Doi, Morizane et al. 2012). Based on this work, the relation between level of differentiation and survival appears to be more complicated with astrocytes, as hiPSC-NSCs fared better than any of the treated cells, but of the treated cells, the most mature BMP4-generated astrocytes survived best. Further experiments, including those using cells treated with combinations of the three cytokines, are required to determine the governing principles of astrocyte differentiation and transplantation.

Other future studies should address the comparative efficiency of astrocyte generation in other hiPSC lines. While hESCs and hiPSCs are similar in many respects, they can vary substantially in their ability to terminally differentiate into a particular neural cell type (Hu, Weick et al. 2010; Tokumoto, Ogawa et al. 2010). Thus, it is important to remember that results from one cell type may not necessarily hold for another, even when comparing hiPSC lines to one another (Hu,

Weick et al. 2010). This is an important implication for clinical translation of hiPSC technology since cells may vary dramatically from patient to patient.

Conclusion

While efficient induction of neural cells could be accomplished in multiple pluripotent stem cell lines via multiple methods, generation of astrocytes proved more challenging. Long term *in vitro* expansion was necessary, and only one cytokine (BMP4) resulted in mature astrocyte marker expression. Further transplant of hiPSC-derived astrocytes in the adult spinal cord was only modestly successful, highlighting the need for further refinement of differentiation and transplantation techniques in order to realize the therapeutic potential of patient-derived astrocytes and their progenitors for CNS disorders.

CHAPTER III: Caudalized human iPSC-derived neural progenitor cells replace neurons and glia but do not restore behavioral function in a chronic cervical spinal cord injury model

Summary

Neural progenitor cells (NPCs) have shown modest potential and some side effects (e.g. allodynia) for treatment of spinal cord injury (SCI). In only a few cases, however, have NPCs shown promise at the chronic stage. Given the 1.275 million people living with chronic paralysis, there is a significant need to rigorously evaluate the cell types and methods for safe and efficacious treatment of this devastating condition. For the first time, I examined the pre-clinical potential of NPCs derived from human induced pluripotent stem cells (hiPSCs) to repair chronic SCI. hiPSCs were differentiated into region-specific (i.e. caudal) NPCs, then transplanted into a new, clinically relevant model of chronic cervical SCI. I established the conditions for successful transplantation of caudalized hiPSC-NPCs and demonstrate their remarkable ability to integrate and produce multiple neural lineages in the chronic injury environment. In contrast to prior reports in acute and sub-acute injury models, survival and integration of hiPSC-derived neural cells in the chronic cervical model did not lead to significant improvement in forelimb function. These data indicate that while hiPSCs show promise, future work needs to focus on the specific hiPSC-derivatives or co-therapies that will restore function in the chronic injury setting.

Introduction

Spinal cord injury (SCI) destroys neural and glial elements and severs the axonal connections between the motor and sensory systems leading to permanent and often devastating loss of function (Schwab and Bartholdi 1996). In recent decades, the therapeutic promise of replacing lost neurons and glia by transplantation has gained significant momentum and even garnered the development of clinical trials (Fehlings and Vawda 2011). Neural stem and progenitor cells comprise a promising resource for the treatment of traumatic spinal cord injury. A number of studies have demonstrated the ability of human neural progenitor cells (NPCs) to promote functional recovery (Ogawa, Sawamoto et al. 2002; Cummings, Uchida et al. 2005; Hofstetter, Holmstrom et al. 2005; Iwanami, Kaneko et al. 2005; Okada, Ishii et al. 2005; Salazar, Uchida et al. 2010). NPCs derived from human embryonic and induced pluripotent stem cells (hiPSCs) have also shown efficacy (Keirstead, Nistor et al. 2005; Kumagai, Okada et al. 2009; Nori, Okada et al. 2011; Fujimoto, Abematsu et al. 2012). NPCs derived from hiPSCs (hiPSC-NPCs) offer particular advantages over those from other cell types and tissues, including reduced need for immunosuppression (as cells are autologous) and obviating ethical concerns. The former is of particular importance to SCI patients, as they are prone to opportunistic infections (Nash 2000), and an immunosuppressive regime would compound their vulnerability.

Interestingly, almost all of the studies cited above target the acute and subacute time points for intervention, transplanting at 9 days post-injury or sooner. Such models, however, are of limited value to the 1.275 million patients currently living with chronic spinal cord injury (CDRF 2009). There are only two published studies to date utilizing human cells in chronic spinal cord injury. The first study transplanted human embryonic stem cell (hESC)-derived oligodendrocyte

precursor cells at 10 months after injury and found no improvement in functional recovery (Keirstead, Nistor et al. 2005). The second study reported an improvement in locomotor recovery when human fetal brain neural stem cells (NSCs) were transplanted 30 days after injury (Salazar, Uchida et al. 2010). This improvement, however, was only statistically significant when compared to vehicle injection, and no difference was observed between the human NSCs and human fibroblasts. Thus the appropriate cell population, conditions and co-therapies for the treatment of chronic spinal cord injury have yet to be identified.

The cervical region is the most commonly affected in spinal cord injury (approximately 50-60% of human SCI (National Spinal Cord Injury Statistical Center 2011)), and contusion is the most common type of injury (Sekhon and Fehlings 2001). Further, regaining function in the hands and arms is the most critical determinant of quality of life for quadriplegic patients (Anderson 2004). Thus for the present study I developed a chronic cervical contusion injury that replicates many of the motor and sensory functional deficits seen in humans. I then examined the ability of hiPSC-NPCs to integrate into the injury environment and characterized their survival and ability to generate neuronal phenotypes. I conferred posterior identity to hiPSC-NPCs through the use of retinoic acid, which induced uniform expression of the hindbrain/spinal cord-specific homeobox gene HoxB4. Though hiPSC-NPCs survived for two months, integrated and differentiated into neurons and glia, this did not translate into measurable functional improvement.

Materials and Methods

Cell Culture

hiPSCs were generated from human fetal lung fibroblasts (IMR90) as previously described(Suhr, Chang et al. 2009). To generate hiPSC-NSCs, colonies were separated from their feeder layer and cultured in suspension for 10 days in DMEM:F12 and N2. The resultant embryoid bodies were then plated on poly-ornithine/laminin and observed for formation of neural tube-like rosettes. Colonies containing rosettes were then detached mechanically and grown in suspension in medium consisting of DMEM:F12, N2, retinoic acid (RA, 1 μM) and basic fibroblast growth factor (bFGF, 10 ng/ml). On day 22, sonic hedgehog (100 ng/ml) was added, and on day 29 cAMP (1 μM) was added to the medium. From day 32 onward, cells were maintained in DMEM:F12, N2, cAMP, T3 (60 ng/ml), platelet-derived growth factor-AA (PDGF-AA, 10 ng/ml), insulin-like growth factor 1 (IGF-1, 10 ng/ml) and neurotrophin-3 (NT3, 10 ng/ml). IMR90 fibroblasts were cultured in DMEM containing 10% fetal bovine serum (FBS) and grown to confluence prior to transplant.

To obtain a single cell suspension, cells were treated with Accutase for 5-10 min, pelleted and resuspended in a PBS solution containing 5 mM glucose and 0.1 mg/ml DNase at a concentration of 100,000 cells/μl.

MRC5c3 hiPSCs were generated using MRC5 fibroblasts (ATCC) and Oct4-Sox2 and Nanog-Lin28 vectors (Addgene). Fibroblasts were exposed to 25 μl of each virus for 4-6 hours (day 0). Cells were plated on day 6 in hESC medium (DMEM:F12, 20% KnockOut(™) Serum Replacement, 4 ng/ml bFGF) on a feeder layer of mouse embryonic fibroblasts. Colonies were

picked days 21-28. MRC5c3 hiPSCs were differentiated to the rosette stage as described for IMR90 hiPSCs.

Immunofluorescence (Cells)

After fixation with 4% paraformaldehyde for 20 minutes, the cells were incubated with 10% donkey serum for 1 hour, then incubated in primary antibodies overnight at 4ºC. After a PBS wash and incubation with secondary antibodies at RT for 2 hours, nuclei were counterstained with 4',6-diamidino-2-phenylindole (DAPI) and mounted.

TaqMan Low-Density Array Analysis

Total cellular RNA was isolated from each of four cell populations (hESCs, IMR90 hiPSCs, hiPSC-NPCs and IMR90 fibroblasts) with the RNeasy Mini Kit (Qiagen). mRNA expression was analyzed using the custom TaqMan low-density array fluidic card following the manufacturer's protocol.

Animals and Surgeries

Adult female Long-Evans rats were used in this study. Animals were 8 weeks old at initiation of training and approximately 5 months old at time of injury.

Animals received intraperitoneal injections of 80 mg/kg ketamine and 15 mg/kg xylazine. A laminectomy was performed at the C4 spinous process of the lamina ipsilateral to the animal's dominant paw (determined via behavioral tasks described below).

The animals were then placed in a spinal frame and a contusion injury was conducted using a fourth generation Ohio State Injury Device (Horner and Stokes 1995). An electromagnetically controlled probe (0.7 mm end diameter, Ling Dynamics, Inc) was lowered to the surface of the cord just lateral to midline. The probe was oscillated on the surface of the spinal cord to achieve

a common starting force of 3000 kilodynes for all animals. The spinal cord was displaced 0.8 mm for 14 msec to induce the injury. The surgical site was closed by suturing muscle in layers and closing skin with wound clips.

Four weeks after injury, scores on the forelimb reaching task (FRT, see below) stabilized, allowing for tight control for injury severity prior to transplantation. Thus, animals were assigned to treatment groups based on FRT such that all groups had equal average scores. All animals received transplants or control procedures at four weeks after injury. One group receiving hiPSC-NPCs (n=7) was followed for four weeks. The remaining animals were assigned to receive hiPSC-NPCs (n=11), IMR90 fibroblasts (n=9), PBS (n=8) or sham transplantation (n=10) and were followed for eight weeks.

In preparation for transplantation, animals were anesthetized and the injury site exposed. After placement in a spinal frame, a pulled glass capillary (OD 70-100 μm) was placed on the lateral border of the gray matter and stereotactically lowered to a depth of 1.0 mm, targeting the gray-white border of the dorsolateral funiculus. Animals in the hiPSC-NPC and fibroblast groups received two injections of 100,000 cells each (1.0 μl injected over 60 s), one rostral and one caudal to the injury site. The PBS group received two 1 μl injections, while sham animals were suspended in the frame but received no injection. Muscles were subsequently sutured in two layers and the skin closed. All animals received daily subcutaneous injections of cyclosporine (10 mg/kg, Sandimmune) from the day of transplant to the time of sacrifice.

Tissue Processing

Animals were anesthetized and perfused transcardially with saline followed by 4% paraformaldehyde (PFA) in 0.1M phosphate buffer. Spinal columns were post-fixed overnight,

cryoprotected with 30% sucrose, and then cut into five 1-mm coronal sections surrounding the lesion, embedded in OCT medium and flash frozen. 20 µm sections were cut on a Leica CM1850 cryostat in a one-in-six series and stored at -80ºC.

Immunofluorescence (Tissue)

Tissue was permeabilized with 0.4% Triton, then blocked with 5% donkey serum (DKS) and 0.4% Triton. Primary antibodies were applied to sections at 4˚C overnight. Slides were then rinsed 3 times in PBS, and incubated in the appropriate secondary antibody solution overnight at 4˚C. Sections were rinsed twice more with PBS, then incubated with DAPI before mounting.

Antibodies

The following antibodies were used: Dcx (Santa Cruz, 1:100), GFAP (Millipore, 1:2000), GSTpi (Millipore, 1:500), hGFAP (StemCells, Inc., 1:1000), HoxB4 (Developmental Studies Hybridoma Bank, 1:100), HuNu (Millipore, 1:300), Ki-67 (Abcam, 1:500), MBP (Millipore, 1:500), Sox9 (R&D Systems, 1:500), and TuJ1 (Covance, 1:1000).

To determine cell survival, stereology was conducted using a Zeiss Axioplan microscope and StereoInvestigator software (MBF Biosciences). Survival of human cells was quantified by HuNu (Millipore) immunolabeling with the optical disector probe and systematic random sampling according to stereological principles.

For quantification of hiPSC-NPC phenotypes *in vivo*, imaging of 15 sections per animal was performed on a Nikon Confocal microscope. A minimum of 100 HuNu+ cells per animal were counted, as were the numbers of human cells expressing GSTpi, GFAP, or Dcx, and percentages of HuNu-positive cells for each were calculated.

Limb-Use Asymmetry Test

The limb-use asymmetry test (LUAT) was used to assess forelimb preference during vertical exploration in a clear Plexiglas cylinder. Animals were scored by blinded observers on independent and simultaneous use of their left and right forelimbs when rearing to make wall contacts (Schallert, Fleming et al. 2000; Gensel, Tovar et al. 2006). Each session lasted until an animal made 20 wall contacts. To determine the degree to which animals preferred their unaffected forelimb after injury, an asymmetry score was calculated for wall contacts for each test session, *asymmetry = [(affected forelimb) + .5(both forelimbs)]/20*, with a score below 0.5 indicating preference for the unaffected forelimb. No training is required for this test, and all animals prior to injury were close to a score of 0.5, indicating no paw preference (average 0.4875 ± 0.08 SD)

Forelimb Reaching Task

The forelimb reaching task was used to assess skilled reaching ability (Alaverdashvili and Whishaw 2010). Animals were trained to extend their forelimb through a slot in a clear Plexiglas box to grasp and eat a chocolate-flavored 35 mg precision-ground food pellet (Bioserv).

In a series of 10-minute sessions, animals were first introduced to the food pellets and testing box, and gradually trained to reach through the slots to grasp pellets. Once animals showed a clear preference for reaching with either the left or right paw, the slot corresponding to the other paw was blocked off and animals were allowed to reach with only their preferred paw. Animals were trained until they were reaching consistently with a success rate ~70% (approximately 3 months training for all animals).

Throughout the experiment, animals were tested for 10 minutes or until they completed 20 trials. A trial was defined as any advance of the paw towards the pellet, concluding when the animal

moved the pellet off of the indentation with its paw or left the front of the box. Experimenters blind to treatment groups recorded total successes, successes on the first attempt, and failures. A trial was considered successful when an animal grasped the pellet with the appropriate paw, transported it into the box, and placed it into its mouth without allowing the pellet to touch the floor.

Statistical Analysis

For each treatment group, the difference in LUAT scores at 3 weeks post-injury and 8 weeks post-transplant was compared using a paired two-tailed t-test. All errors are SEM unless otherwise indicated.

Study Approval

All animal-related procedures were approved by the Institutional Animal Care and Use Committee of the University of Washington and were conducted in accordance with the guidelines of the NIH.

Results

Human induced pluripotent stem cells generate neural stem cells and can be further differentiated into specific neural lineages

I tested the ability of hiPSCs to first form neuroepithelial stem cells, and then further differentiate into cells of neural lineages. The differentiation protocol is outlined in Fig. 1a. After two weeks, hiPSC colonies contained radially-oriented columnar cells that formed neural tube-like rosettes (Fig. 1b). After 45 days, adherent aggregates produced TuJ1-positive neurons and

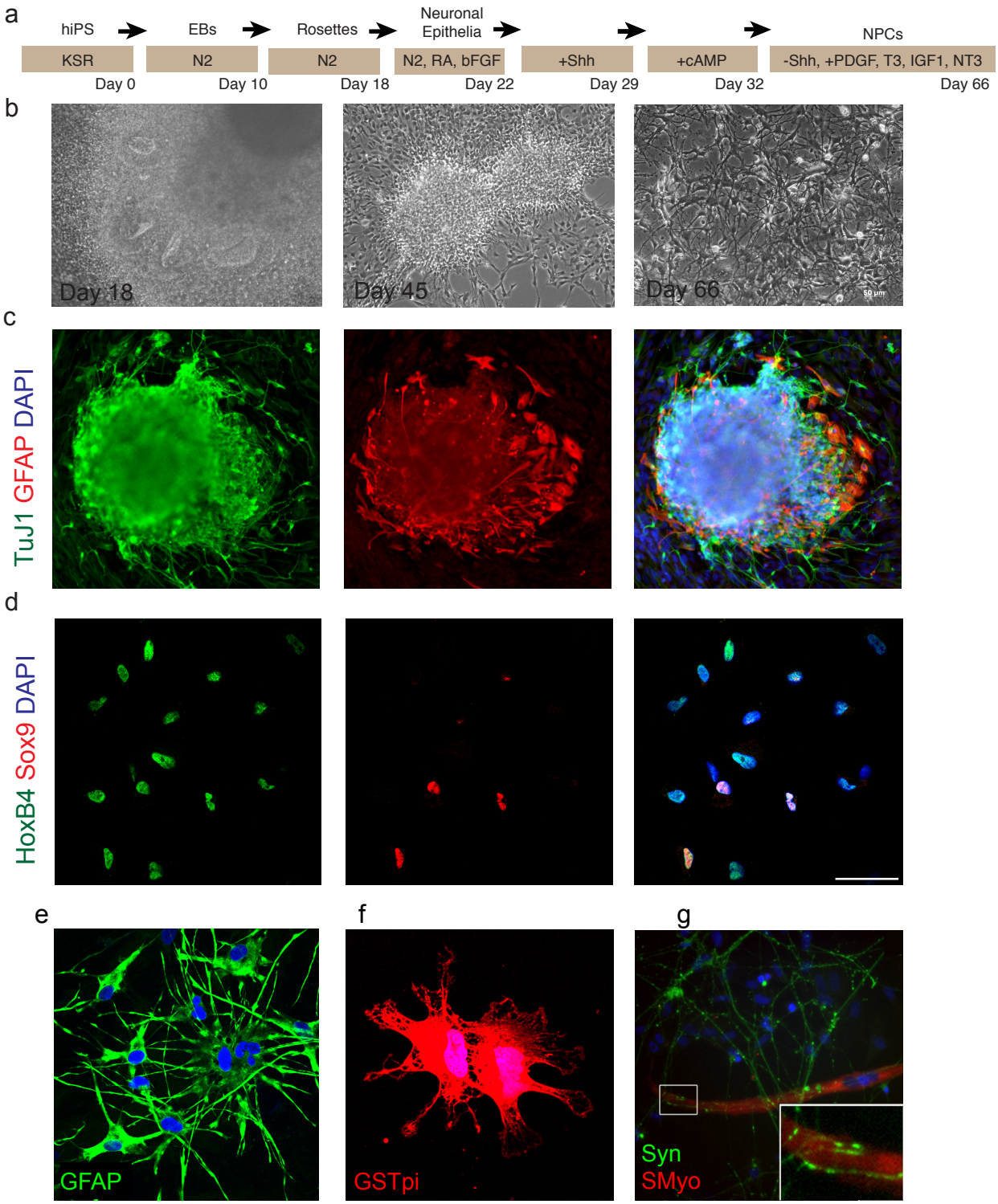

Figure 1 | hiPSCs form region-specific neural progenitor cells. a, Outline of differentiation protocol. **b**, Morphological characteristics of differentiated hiPSCs. **c**, At day 45, hiPSCs expressed the neuronal marker TuJ1 and the astrocyte marker GFAP. **d**, hiPSC-NPCs uniformly express HoxB4,and demonstrate expression of Sox9. **e**, Most hiPSC-NPCs express GFAP. **f**, A small subset of hiPSC-NPCs express the oligodendrocyte marker GSTpi. **g**, When co-cultured with RMT fibers, hiPSC-NPCs express synapsin and are observed in close association with muscle fibers (inset). Scale bars = 50 µm.

GFAP-positive astrocytes (Fig. 1c). Prior to transplantation, hiPSC-NPCs formed a monolayer displaying complex progenitor morphologies.

The caudalizing factor retinoic acid (RA) was included during differentiation to induce the expression of the hindbrain/spinal cord-specific transcription factor HoxB4 (Bass and Baker 1997; Hu and Zhang 2009) (Fig. 1d). A small percentage (9.8 ± 2.2%) remained Sox9-positive (Fig. 1d), a marker of neural stem cells (Cheng, Pastrana et al. 2009; Scott, Wynn et al. 2010) and an essential component of the developmental switch from neurogenesis to gliogenesis (Stolt, Lommes et al. 2003; Kang, Lee et al. 2012). In contrast, another hiPSC line differentiated only to the neuronal epithelial stage was uniformly HoxB4-positive, but expressed much higher levels of Sox9 (94.7 ± 2.1%) (Fig. 2).

A very high percentage of hiPSC-NPCs displayed a stellate morphology and weakly expressed the astrocytic marker GFAP (Fig. 1e). A smaller proportion expressed the mature oligodendrocyte marker GSTpi (Fig. 1f). These cells exhibited morphologic characteristics of oligodendrocytes, including membranous sheets with lacy appearances (Dyer and Benjamins 1989; Dyer and Benjamins 1989). A subset of cells also expressed mature neuronal markers including neurofilament, vesicular acetylcholine and synapsin (data not shown). Further, when co-cultured with sMyo-positive RMT myofibers, synapsin-positive hiPS-NPCs were observed in close association with the muscle fibers (Fig. 1g), suggesting the ability to make the physical contact necessary to form a neuromuscular junction.

hiPSC-NPCs express decreased levels of pluripotency genes and increased levels of neural genes

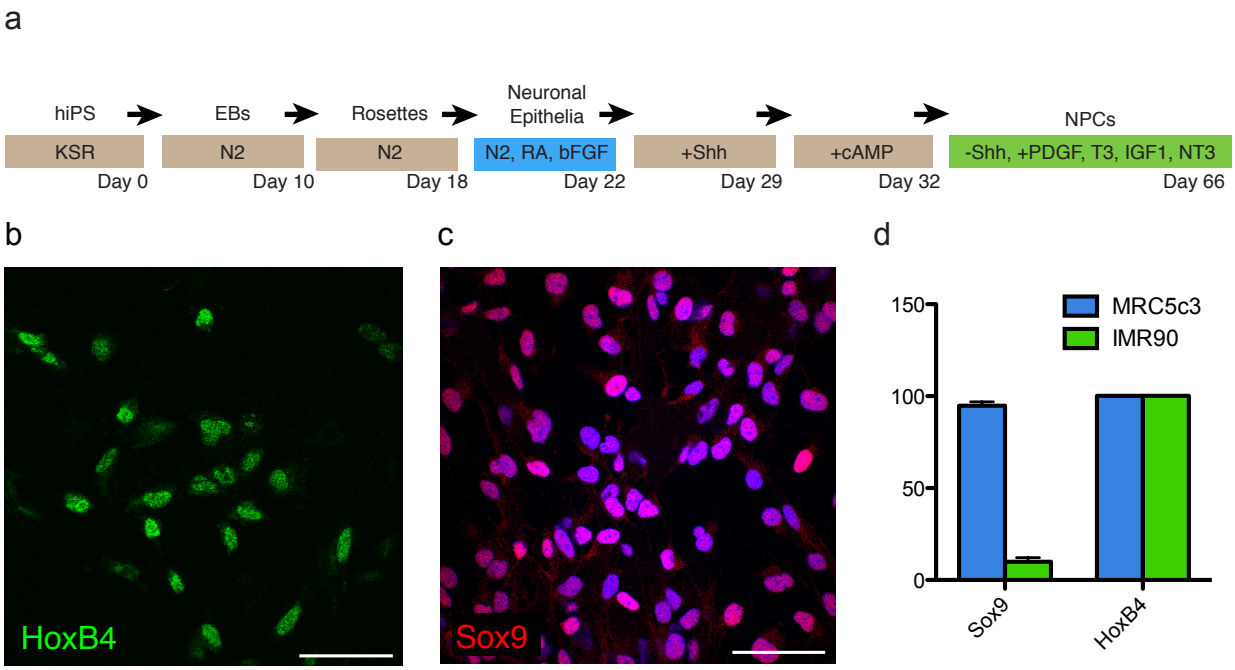

Figure 2 | hiPSCs form region-specific neural progenitor cells. a, Outline of differentiation protocol. MRC5c3 hiPSCs (blue) were induced to form neural rosettes, while IMR90 hiPSCs (green) were further differentiated down a progenitor lineage for transplantation. **b-c**, At the neuronal epithelia stage, MRC5c3 hiPSC-NSCs uniformly expressed the hindbrain homeobox gene HoxB4 (**b**) and the neural stem cell marker Sox9 (**c**). **d**, Quantification of HoxB4 and Sox9 in caudalized IMR90 hiPSC-NPCs and MRC5c3 NSCs. Scale bars = 50µm.

To further characterize hiPS-NPCs, TaqMan low-density array (LDA) analysis was performed, with hESCs, undifferentiated IMR90 hiPSCs and IMR90 fibroblasts (FIB) serving as controls. Compared to both hESCs and hiPSCs, hiPS-NPCs expressed significantly lower levels of several pluripotency markers, including LIN28, NANOG, POU5F1(OCT4), and UTF1 (Fig. 3a). hiPS-NPCs also expressed lower levels of telomerase, a reverse transcriptase important in maintaining telomere length, compared to pluripotent cells. Meanwhile, hiPS-NPCs displayed upregulated levels of neural stem cell markers PAX6 and SOX9. As expected, high levels of SOX2 were observed in hESCs, hiPSCs and hiPS-NPCs compared to fibroblasts. SOX2 is a transcription factor essential in maintaining self-renewal and pluripotency of undifferentiated hESCs (Adachi, Suemori et al. 2010) and one of the key transcription factors required in hiPSCs (Zhao and Daley 2008). It is also a marker for multipotent neural stem cells (Ellis, Fagan et al. 2004).

hiPS-NPCs generally expressed elevated levels of genes specific to cells of neuronal and glial lineages as well. For neurons, these included doublecortin (DCX*)*, microtubule-associated protein 2 (MAP2), neural cell adhesion molecule 1 (NCAM1), and neuropeptide Y (NPY) (Fig. 3b). hiPS-NPCs also expressed neuron-specific enolase (ENO2) and glutamic acid decarboxylase (GAD1), though levels were comparable to pluripotent cell types.

Neural induction of hiPSCs resulted in upregulation of several astrocyte markers (Fig. 3c), most notably glial fibrillary acidic protein (GFAP), consistent with the expression seen in Fig. 1e. Caudalized hiPSC-NPCs were also the only cell type to detectably express the immature astrocyte marker S100β, the astrocyte-specific glutamate transporter SLC1A2, and HES5, a transcription factor thought to regulate astrocyte v. neuron fate of neural stem cells. The intermediate filament vimentin (VIM) was expressed at the highest levels by hiPS-NPCs, though

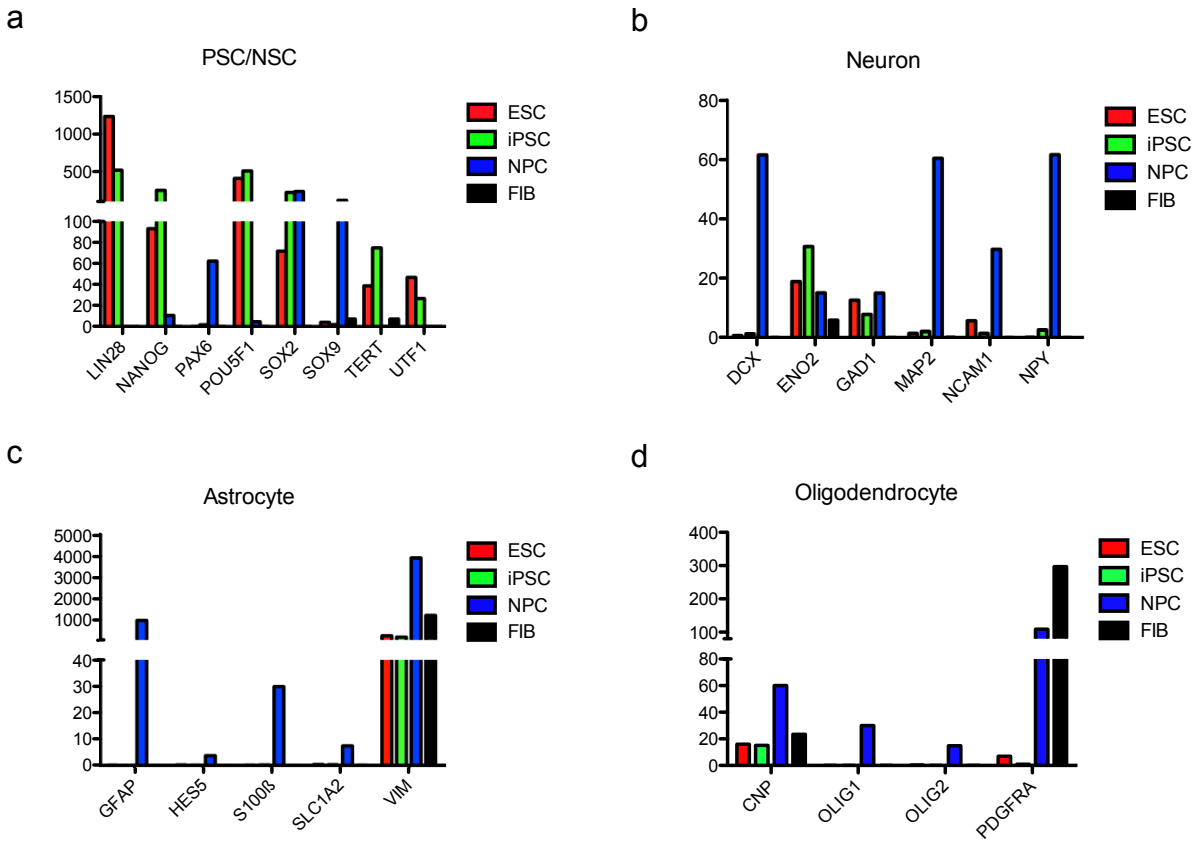

Figure 3 | Caudalized hiPSC-NPCs downregulate pluripotency genes and broadly upregulate neuron and glial specific genes.
TaqMan low-density array data is arranged by pathway. **a**, Pluripotent stem cell and neural stem cell markers. ESCs and hiPSCs expressed high levels of pluripotency markers, while hiPSC-NPCs downregulated these same genes and dramatically elevated expression of the neural stem cell markers PAX6 and SOX9. **b**, Neuronal markers. hiPSC-NPCs expressed elevated levels of neuron-specific transcripts including DCX, MAP2, NCAM1 and NPY compared to pluripotent ESC or iPSC controls. **c**, Astrocyte markers. hiPSC-NPCs expressed dramatically higher levels of GFAP and S100β and modest elevation of SLC1A2. **d**, Oligodendrocyte markers. hiPSC-NPCs expressed many genes of the oligodendrocyte lineage, including CNPase and PDGRα. OLIG1 and OLIG2 were uniquely expressed in hiPSC-NPCs when compared to pluripotent stem cell controls.

all four cell types expressed high levels of this marker. Within the nervous system, vimentin is typically used as an immature or reactive astrocyte marker, though it is also expressed by many other cell types throughout the body and thus is not expected to be CNS-specific.

Oligodendrocyte lineage markers expressed by hiPS-NPCs included CNPase (CNP), olig1, and olig2 (Fig. 3d). The platelet-derived growth factor receptor PDGFRα, an oligodendrocyte precursor cell marker, was also expressed at very high levels compared to pluripotent cell types, though somewhat lower than fibroblasts, which are also known to express this receptor.

Unilateral cervical contusion results in cavitation, extensive myelin loss and gliosis

To create a clinically relevant model of cervical spinal cord injury, I adapted a fourth generation Ohio State SCI Device (Fig. 4a). Animals received a unilateral C4 contusion injury on the side of the spinal cord corresponding to the dominant forelimb, as determined by training on the forelimb reaching task.

Histologic signs of traumatic injury in this model occur primarily in the dorsolateral funiculus, where the lesion epicenter includes substantial cavitation, widespread loss of myelin in the lateral white matter, and a rim of reactive astrocytosis surrounding the lesion cavity (Fig. 4b) In contrast to midline thoracic contusions, which typically display considerable mediolateral extension, cavitation and signs of cellular loss in this model are limited to the side of injury.

Up to 8 weeks after transplantation, caudalized hiPSC-NPCs had survived and integrated into the injured spinal cord. The average number of cells per animal was 169,126 ± 65,359. Most cells were found in juxtaposition to the lesion cavity, however, cells could be observed throughout the injured hemicord (Fig. 4d). Caudalized hiPSC-NPCs were observed in the gray matter, in the dorsal columns and the ventral white matter, with some cells in close proximity to the ventral pia

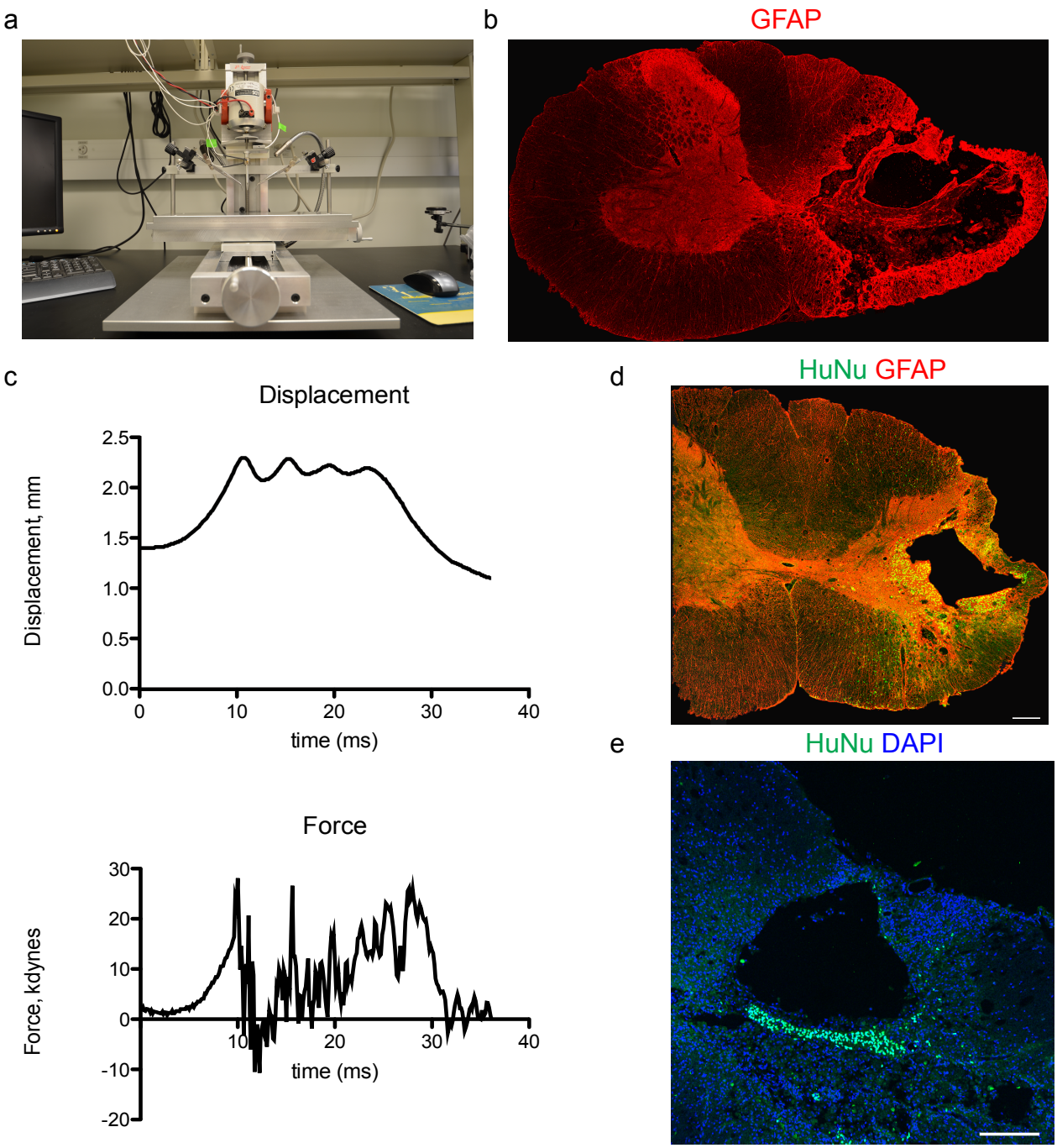

Figure 4 | A chronic cervical hemi-contusion model that recapitulates human pathology. **a**, Fourth generation of the OSU injury device. **b**, Four weeks after injury, GFAP staining reveals substantial cavitation and reactive gliosis on the side of contusion. **c**, Contusion injury data: representative displacement and force tracings from one injury. **d**, Eight weeks after transplant, hiPSC-NPCs have survived and integrated in the chronic contusion model. Most cells remain close to the site of injection (i.e. near the gray-white border of the dorsolateral funiculus and juxtaposed to the lesion cavity), but many migrated throughout the ipsilateral white and gray matter. **e**, IMR90 fibroblasts eight weeks after transplant. Scale bar = 200 μm in **d**, 100 μm in **e**.

mater. No cells were observed on the contralateral side of the spinal cord, though some could be found near the anterior median fissure.

hiPSC-NPCs continue to divide and form neurons and astrocytes in the chronically injured cord 4 weeks after transplant

Four weeks after transplantation, some transplanted cells expressed Ki-67 (Fig. 5a), a protein strictly associated with proliferation (Scholzen and Gerdes 2000). Many caudalized hiPSC-NPCs stained positively for a human-specific GFAP marker (hGFAP) (Fig. 5b), while none were observed to express MBP. In fact, hGFAP+ cells were often well-demarcated from MBP+ regions of the cord, demonstrating relatively little physical contact between transplanted cells and myelin.

Very rarely, I observed a HuNu+ cell expressing doublecortin (Fig. 5c), a microtubule-associated protein expressed by neuronal precursor cells and retained during early neuronal maturation (Brown, Couillard-Despres et al. 2003). Orthogonal views confirm the association of doublecortin and the neurogenic capacity of transplanted hiPSC-NPCs in the chronically injured cord. HuNu+/Dcx+ cells also expressed the pan-neuronal marker β-tubulin, as did many HuNu+/Dcx- cells (data not shown), providing further evidence for neurogenesis by caudalized hiPSC-NPCs.

While less than 10% of hiPSC-NPCs were Sox9+ *in vitro*, a much higher percentage expressed the marker *in vivo* (Fig. 5d), suggesting either a selection for - or acquisition of - this phenotype in the spinal cord.

hiPS-NPCs form neurons, astrocytes and oligodendrocytes 8 weeks after transplant

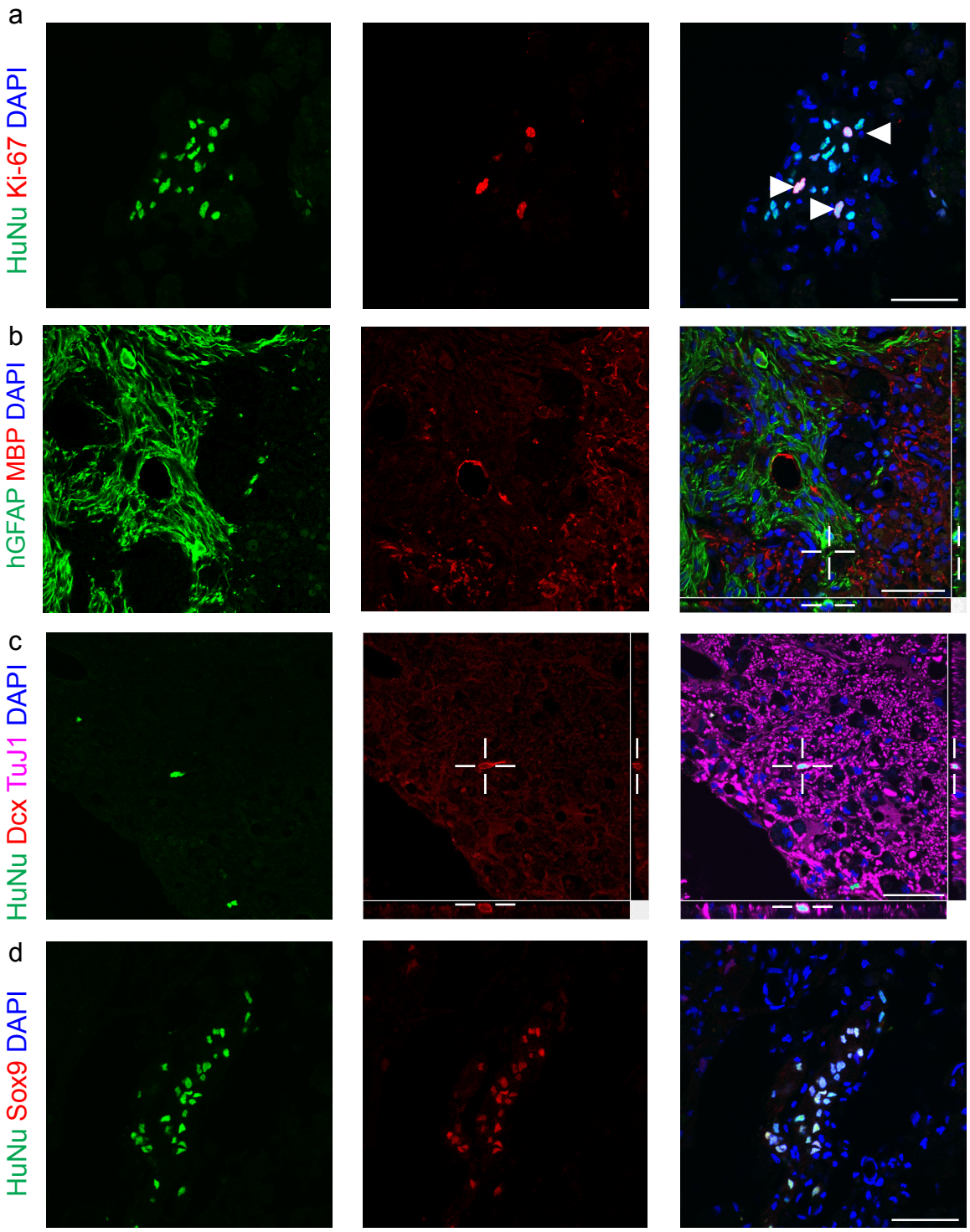

Figure 5 | Caudalized hiPSC-NPCs four weeks after transplant divide and express Sox9. a, A percentage of HuNu-positive cells also express the proliferation marker Ki-67. Arrowheads indicate HuNu/Ki-67 double-positive cells. **b**, NPCs are positive for a human-specific GFAP antigen, but do not express MBP. **c**, Exogenous formation of immature neurons is rare after four weeks. Z-stack merge confirms colocalization of Dcx with HuNu. **d**, A higher percentage of NPCs express Sox9 in vivo than in vitro. Scale bars = 50µm.

Eight weeks after transplantation, a high percentage of transplanted cells near the injury cavity expressed the neuronal marker β-tubulin (Fig. 6a). A subset of these also expressed doublecortin (11.4 ± 3.0%), and some HuNu+/Dcx+ cells displayed bipolar morphologies consistent with those of newly generated migrating neurons.

A large percentage of transplanted cells expressed glial markers as well (Fig. 6c), including GFAP (49.1 ± 1.2%) (Fig. 6d) and the oligodendrocyte marker GSTpi (17.2 ± 2.4%) (Fig. 6e). No Ki-67+ cells were detected at this time point, suggesting that hiPSC-NPCs were no longer dividing 8 weeks after transplant.

Behavioral analysis indicates no improvement in grasping or weight-bearing ability after hiPSC-NPC transplantation compared to sham controls

Despite thorough integration and differentiation into both neurons and glia, assessment of behavioral recovery indicates that transplantation of hiPS-NPCs did not confer significant improvement on either the forelimb reaching task (Fig. 7a) or the limb-use asymmetry test (LUAT) (Fig. 7b). Neither the hiPSC-NPC group nor any of the control groups exhibited improvement on the FRT. Animals in the hiPSC-NPC and sham group showed statistically significant improvement in their LUAT scores (hiPSC-NPC: $p=0.0092$, sham: $p=0.0032$) (Fig. 7c). Animals receiving either PBS or IMR90 fibroblasts demonstrated little change in their paw preferences. Comparisons across groups are not valid for the LUAT, as treatment assignments were based on FRT scores, thus the average performance on the LUAT was not similar across groups prior to transplant.

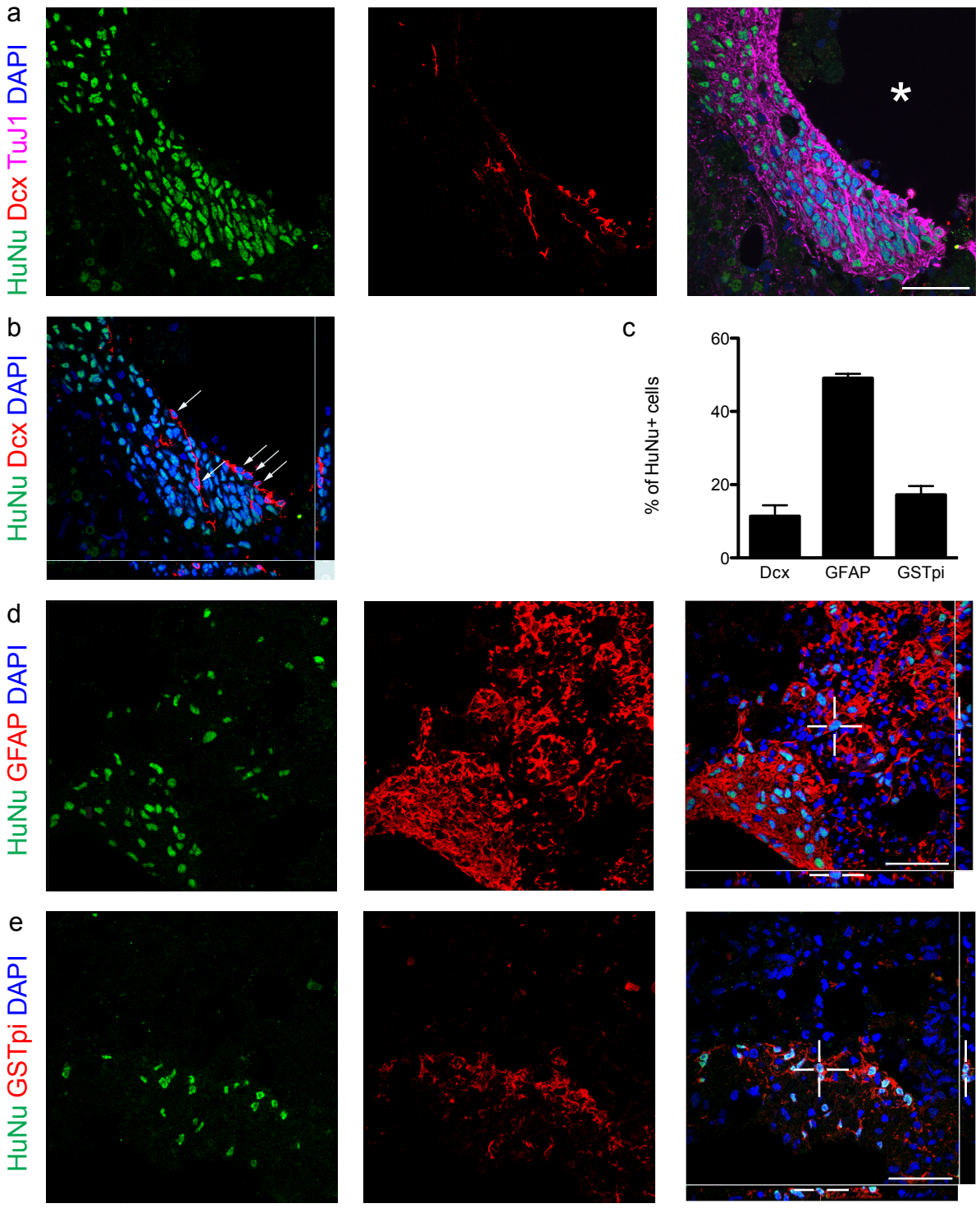

Figure 6 | Caudalized hiPSC-NPCs eight weeks after transplant stop dividing and differentiate into neurons and glia. a, HuNu-positive cells adjacent to the lesion cavity (asterisk) express the immature neuronal marker doublecortin and the pan-neuronal marker TuJ1. **b**, Z-stack imaging of Dcx-positive hiPSC-NPCs (arrows) confirms neurogenesis in the injured spinal cord. **c**, Phenotypic analysis of hiPSC-NPCs shows the percentages of Dcx-positive neurons, GFAP-positive astrocytes and GSTpi-positive oligodendrocytes. **d**, A portion of NPCs retain expression of GFAP. **e**, Some NPCs have differentiated into GSTpi-positive oligodendrocytes. Error bars are SEM. Scale bars = 50 µm.

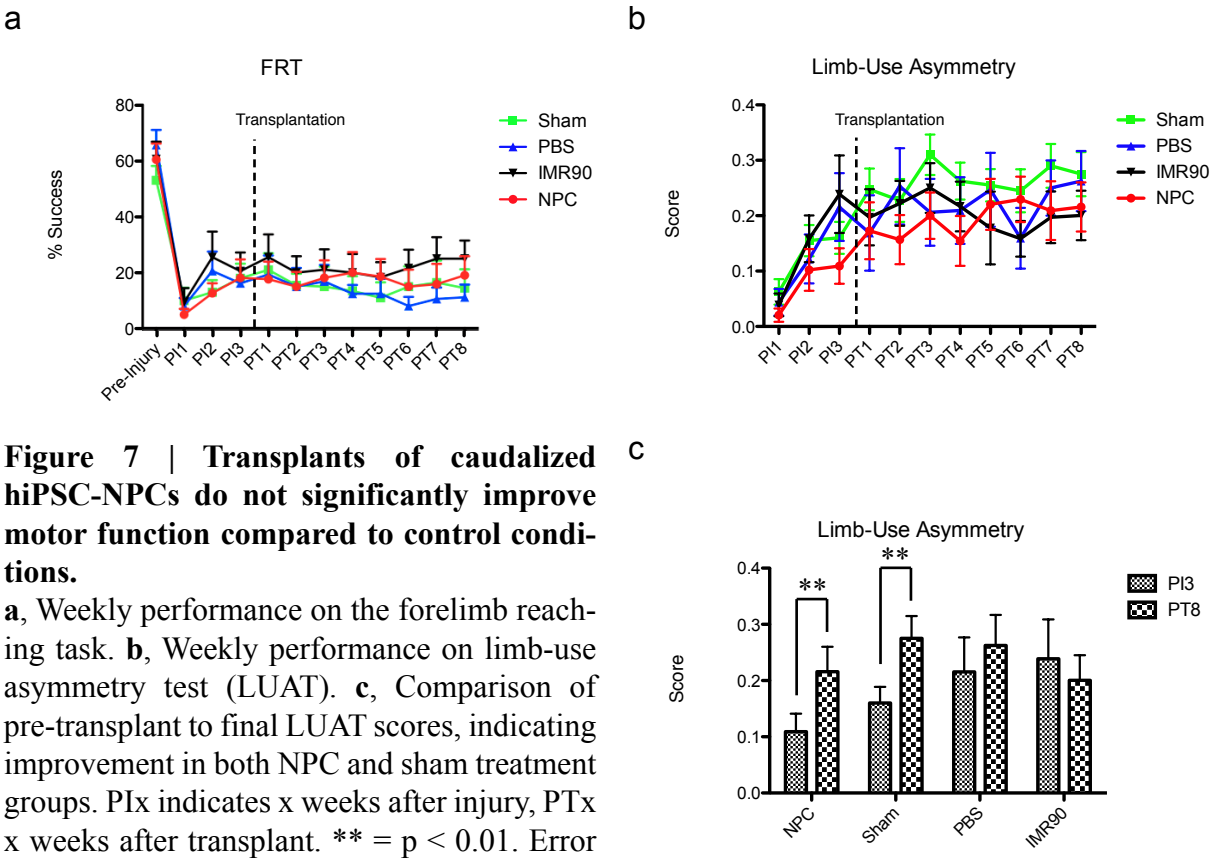

Figure 7 | Transplants of caudalized hiPSC-NPCs do not significantly improve motor function compared to control conditions.

a, Weekly performance on the forelimb reaching task. **b**, Weekly performance on limb-use asymmetry test (LUAT). **c**, Comparison of pre-transplant to final LUAT scores, indicating improvement in both NPC and sham treatment groups. PIx indicates x weeks after injury, PTx x weeks after transplant. ** = $p < 0.01$. Error bars are SEM.

Discussion

Neural transplantation shows great promise for promoting cell replacement and plasticity, particularly in the acute and sub-acute period following spinal cord injury. Treatment of the chronically injured spinal cord has proven significantly less tractable. Research efforts have been limited, in part due to the scientific challenges of working with chronic animal models of scarring and a decreased inherent plasticity of the aging nervous system. But there are also practical limitations that have left this clinical population underserved, including the exceptionally demanding laboratory time and cost of conducting large-scale, blinded studies in chronic animal models. Here I developed a chronic model of cervical SCI which mimics many of the clinical characteristics of human cervical injury. I focused on the development of an exciting new cell engineering technology, hiPSCs, to create a potentially autologous source of NPCs to use as transplantable resource for neural cell replacement. To my knowledge, this is the first study describing the transplantation of hiPSC-NPCs into the chronically injured spinal cord. These studies indicate that caudalized hiPS-NPCs develop into multiple neural lineages that survive for up to two months post-transplant without risk of overgrowth or loss of function.

The injury model developed corresponds closely to the most common forms of spinal cord injury; contusions are the most commonly observed type of spinal cord injury, and the cervical region is the most often injured. A recent systematic review (Tetzlaff, Okon et al. 2011) reported the paucity of data on the transplantation of human cells into chronic cervical models of SCI. This gap in the SCI community's knowledge base is reflected in a recent survey of opinion in which SCI researchers expressed strong support for the demonstration of preclinical evidence of

efficacy in cervical injury models prior to conducting human SCI trials (Kwon, Hillyer et al. 2010).

Further clinical relevance arises from the chronic time point chosen for transplantation, one that is far less frequently studied than acute and sub-acute transplants despite the fact that there are currently 1.275 million people in the U.S. living with chronic SCI. There has been a recent shift among SCI researchers in the criteria for what constitutes a chronic time point, when relative stability in both the injury environment and behavioral recovery is achieved. For humans, this is generally considered to be 12 months post-injury. The corresponding time point in rats is still under debate. Previously, this was thought to occur by about 30 days post-injury (Houle and Tessler 2003; Fawcett, Curt et al. 2007), but recently the field has moved toward defining the threshold for 'chronic' at 6 weeks after injury (Anderson, Beattie et al. 2005). Thus, by transplanting at 4 weeks post-injury, my model may be better characterized as 'early chronic.'

Whereas most studies assessing the efficacy of transplanted cells in spinal cord injury use locomotion to monitor recovery, I chose to observe forelimb function. For human SCI patients, arm use and grasping ability are the important determinants of overall quality of life and independence (Anderson 2004). Even a small recovery in hand function could result in significant benefits. Skilled reaching is useful for assessing injury to motor systems in a more objective manner than locomotion scales. It is also a volitional task that requires greater descending input from the brain compared to locomotor movements, where local spinal circuits may dominate (de Leon, Tamaki et al. 1999; Tillakaratne, Mouria et al. 2000; Tillakaratne, de Leon et al. 2002).

There are many potential approaches to repair of the injured spinal cord through cell therapy. Investigators have transplanted immature neural stem cells, committed progenitors and purified populations of astrocytes, oligodendrocytes and neurons (Ikegami, Nakamura et al. 2005; Mitsui, Shumsky et al. 2005; Karimi-Abdolrezaee, Eftekharpour et al. 2010; Tetzlaff, Okon et al. 2011; Yuan, Martin et al. 2011). In the current work, I established a multipotent neural progenitor population with the capacity to accomplish multiple lineage replacement. I showed that these caudalized hiPSC-NPCs form cells of both neuronal and the two macroglial lineages, astrocytes and oligodendrocytes *in vitro* and *in vivo*.

The key defining features of hiPSC-NPCs include loss of pluripotent stem cell markers, region specificity, and a multipotent NPC phenotype. TaqMan LDA analysis demonstrated the loss of telomerase, the pluripotency marker UTF1, and three of the four reprogramming factors. The hiPSC-NPCs transplanted in this injury model uniformly expressed the hindbrain/spinal cord-specific marker HOXB4, a homeobox protein restricted to the region of the neural tube caudal to the border between rhombomeres 6 and 7 during development. Inclusion of retinoic acid in the differentiation of pluripotent cells is important in conferring this regional specificity (Hu and Zhang 2009). In the results presented above and in work published by other groups, neuralization of hiPSCs without retinoic acid does not confer HoxB4 expression (Hu and Zhang 2009; Krencik, Weick et al. 2011), instead resulting in widespread expression of Otx2, indicating forebrain specificity (Li, Du et al. 2005; Pankratz, Li et al. 2007).

Caudalized hiPSC-NPCs were also largely GFAP-positive and expressed reduced levels of the neural stem cell (NSC) marker Sox9 as compared to cells at earlier stages of differentiation. However, the cells displayed multipotency *in vitro* and *in vivo*, indicating a neural progenitor

phenotype, rather than mature astrocytes. Thus, caudalized hiPSC-NPCs were well-suited to generate neurons and glia in the adult spinal cord without risk of contamination by undifferentiated cells.

Key concerns regarding transplantation into the injured spinal cord are the relative survival of grafted cells (Anderson, Haus et al. 2011) and the potential for overgrowth or tumor formation (Tsuji, Miura et al. 2010; Nori, Okada et al. 2011). There is a dearth of defined practices for striking a balance of controlled survival. Using the protocol I have described here, I found that grafted hiPS-derived neural progenitor cells survived remarkably well when injected juxtaposed to the lesion epicenter of the chronically injured spinal cord. Early attempts at transplantation in a medium of PBS alone, or in PBS+DNase proved unsuccessful (unpublished observations) due to poor cell viability. In the presented work I utilized a solution of DNase and glucose in PBS that proved effective. Cells were well-distributed throughout mediolateral and dorsoventral axes of the ipsilateral hemicord, and found in the white and gray matter. On average, approximately 169,000 cells were detected at 8 weeks after transplant (out of 200,000 injected). As a percentage of cells transplanted, this differs markedly from the study by Salazar et al cited earlier, where transplanting 75,000 human cells at 30 days post-injury resulted in 215,000 cells after 16 weeks, indicating substantial proliferation without apparent deleterious effects. In my work the relative safety of caudalized hiPSC-NPCs is also likely, as no masses were detected and Ki-67 expression reduced to zero by 8 weeks after transplant.

It has been shown that oligodendrocyte progenitor cells are ineffective in chronic injury (Keirstead, Nistor et al. 2005). Neural progenitor cells, however, have shown promise (Cummings, Uchida et al. 2005; Salazar, Uchida et al. 2010) and here I implanted a multipotent

cell capable of creating the three major neural lineages. Interestingly, despite the majority of cells expressing the classic astrocyte marker GFAP prior to transplant, hiPSC-NPCs showed multipotentiality *in vivo*, generating neurons, astrocytes and oligodendrocytes. This plasticity is consistent with recent findings in the field, as several groups have noted the stem cell potential of astrocytes, a capacity augmented by injury (Doetsch 2003; Vaccarino, Fagel et al. 2007; Chong and Chan 2010; Robel, Berninger et al. 2011). The capacity of astroglial cells to also serve as progenitors for neurons and oligodendrocytes enhances their attractiveness as a potential repair resource, since all three main cellular components of the CNS can theoretically be constituted from one cell type. These findings underscore the diversity of roles played by astrocytes, which until recently was under-appreciated.

While <10% of caudalized hiPSC-NPCs were positive for the NSC marker Sox9 prior to transplant, a substantially greater percentage stained positively for Sox9 *in vivo*. The increase in percentage of Sox9+ cells among hiPSC-NPCs after transplant could be attributed to either a selective survival among cells already expressing Sox9 prior to injection, or to acquisition of positivity after transplant. Other groups have observed dramatically reduced survival of fully differentiated hiPSC-derived neural cells as compared to hiPSC-derived stem and progenitor cells (Rhee, Ko et al. 2011; Yuan, Martin et al. 2011), indicating that selective survival is more likely to be the mechanism for the observed change in Sox9 reactivity. The work reported here, however, did not explicitly test this possibility. Future studies including lineage tracing could be helpful in determining which mechanism (selective survival or Sox9 acquisition) is more relevant.

Some important differences in phenotype and proliferation were observed between the 4-week and 8-week time points, indicating that the profile of transplanted cells evolves over a time course on the order of weeks and months. One difference is that Ki-67+ cells were detected at 4 weeks, but not at 8, indicating that proliferation occurred for some time after transplant, but eventually ceased. This is an important consideration, as concerns about the tumorigenicity of hiPSC transplants remain. Though hiPSC-NPCs were differentiated for months prior to transplant, contamination with undifferentiated cells and/or dedifferentiation of NPCs remained potential avenues for tumorigenesis, though no signs of masses or other deleterious effects of overgrowth were observed. Studies in other models of CNS disease such as Parkinson's and stroke have shown masses, neural tube-like rosettes and/or Ki-67+ cells after transplant of hiPSC-derived neural cells (Jensen, Yan et al. 2011; Rhee, Ko et al. 2011), emphasizing the importance of the absence of these features in this study.

Interestingly, the presence of transplanted neural progenitor cells did not translate into myelin repair. By four weeks after transplant, no oligodendrocytes were detected, and grafted cells were well-demarcated from myelinated regions of the cord, despite the fact that almost all NPCs were located in the white matter at this time point. By 8 weeks, 17.1% of NPCs formed GSTpi+ oligodendrocytes, though none could convincingly be demonstrated to form myelin. The lack of myelin repair may correlate with the lack of chronic demyelination (Powers, Lasiene et al. 2012) in that there is not a large population of otherwise intact axons to remyelinate at chronic time points.

Conclusion

These studies demonstrate that hiPS cells can be used to deliver multiple neural cell phenotypes to the chronically injured spinal cord. While I did not observe significant recovery of function, I established a preliminary safety margin of this particular cell type, did not see overgrowth or delayed proliferation and did not detect any decline in function. I followed the transplants for two months, but future studies may need to extend this timeframe and also consider complementary therapies such as physical therapy, electrical stimulation, or growth factor delivery. Interestingly, the number of oligodendrocytes and Dcx+ immature neurons increased from 4 weeks to 8 weeks in this model. Hence, it is reasonable to suspect that hiPSC-NPCs may still have been migrating and differentiating two months after transplant. If this is an indication of continued cell plasticity, then longer follow-up periods or combinatorial therapies to direct transplanted cells are clearly warranted. It is also reasonable to presume that recovery may take longer in the chronic injury setting than in the acute phase, as the injury environment is more dynamic shortly after injury, and it is likely that any endogenous repair mechanisms have concluded after 4 weeks since behavioral recovery has plateaued. In conclusion, hiPS-derived neural progenitor cells show promise as a potential method to introduce cellular plasticity in the chronically injured spinal cord.

CHAPTER IV: Evidence for modest behavioral recovery with a concomitant risk of neural tumors when human iPSC-derived neural stem cells are transplanted into the chronically injured spinal cord

Summary

Human induced pluripotent stem cells (hiPSCs) can be differentiated into neural cells, including neural stem cells and their progeny. My previous work showed that hiPSC-derived neural progenitor cells (hiPSC-NPCs) can be delivered to a chronic cervical rodent model of SCI, where they form neurons and glia but lead to only modest behavioral recovery. I tested the hypothesis that a less mature hiPSC-derived neural stem cell (hiPSC-NSC) would translate to more substantial improvement in forelimb function. At 8-9 weeks after transplant, there was indeed an improvement in performance on the forelimb reaching task, though it was transient. After sacrifice at 15 weeks post transplant, several spinal cords that received hiPSC-NSCs contained large masses. These masses were not teratomas and were comprised predominantly of neural elements. While most concerns about the safety of pluripotent stem cells and their derivatives focus on potential teratomas, here I report the formation of tumors of a strictly neural origin, suggesting that when evaluating stem cell populations for safety, standard teratoma assays may not suffice. This could have important implications for methods of screening hiPSC-derived cells before clinical applications.

Introduction

The advent of human induced pluripotent stem cell (hiPSC) technology has brought the promise of personalized cell-based therapies for treating a wide range of diseases and disorders, including traumatic spinal cord injury (SCI). hiPSCs can differentiate into neural stem cells (NSCs), and in turn into functional neurons and astrocytes (Krencik, Weick et al. 2011; Nori, Okada et al. 2011; Rhee, Ko et al. 2011; Yuan, Martin et al. 2011; Fujimoto, Abematsu et al. 2012). hiPSC-derived NSCs (hiPSC-NSCs) and their progeny can be delivered to acute thoracic models of SCI, where they survive and contribute to locomotor recovery (Nori, Okada et al. 2011; Fujimoto, Abematsu et al. 2012).

However, the prospect of using a pluripotent cell to derive the putative therapeutic cell population brings concerns of tumorigenicity, especially teratoma formation. Several groups have reported teratoma formation after iPSC-derived neural cells were transplanted into the central nervous system (CNS) (Wernig, Zhao et al. 2008; Miura, Okada et al. 2009; Tsuji, Miura et al. 2010). The most likely culprit in these adverse outcomes is the contamination of the transplanted cell population by undifferentiated cells, and indeed reducing or eliminating pluripotent cells prior to transplant is effective in lowering tumor incidence (Wernig, Zhao et al. 2008; Miura, Okada et al. 2009). Embryonic stem cell-based therapies have been plagued by similar risks (Bjorklund, Sanchez-Pernaute et al. 2002; Erdo, Buhrle et al. 2003; Roy, Cleren et al. 2006; Hedlund, Pruszak et al. 2007; Pruszak, Sonntag et al. 2007; Doi, Morizane et al. 2012). All of these studies have focused on the possibility of teratoma formation, while none have reported formation of tumors of other varieties.

My previous work showed that hiPSC-derived neural progenitor cells (hiPSC-NPCs) can be successfully transplanted into a chronic cervical contusion model of SCI, though behavioral improvements 8 weeks after transplant were modest and not significantly better than some controls. Thus I sought to improve on these promising initial results by transplanting less mature hiPSC-NSCs and observing the animals for 15 weeks after cell transplantation. While improvement was detected in animals receiving hiPSC-NSCs on a skilled forelimb task, it did not persist for the duration of the experiment. Processing of spinal cord tissue at the conclusion of the experiment revealed several animals with large intraparenchymal masses. These tumors were not teratomas, suggesting that the etiology of the masses was not contamination with undifferentiated pluripotent cells. The growths were comprised primarily of neural elements, including neurons and glia. These results highlight the need for rigorous safety measures in the evaluation of hiPSC-derived therapies, as teratomas are not the sole concern with these populations.

Materials and Methods

Cell Culture

Undifferentiated IMR90 hiPSCs were obtained from WiCell and grown in TeSR2 (STEMCELL Technologies) on Matrigel (BD Biosciences). hiPSC-NSCs were generated via modification of previously published protocols (Hu and Zhang 2009). On Day 0 of differentiation, colonies are separated from their substrate with 1.925 units/ml dispase and cultured in suspension in T75 flasks in TeSR2 and 10μM Y-27632 dihydrochloride. On Day 4, embryoid bodies (EBs) are switched to a new T75 in neural differentiation medium (NDM: DMEM/F12 containing N2,

MEM non-essential amino acids, 2 μg/ml heparin) and 20 ng/ml FGF. On Day 7, EBs are plated on Matrigel in NDM + FGF. On Day 10, 0.1 μM retinoic acid (RA) is added to the medium. On Day 15, colonies possessing neural tube-like rosettes are mechanically detached using a P1000 pipette and cultured in NBEF (NDM + B27 + 20 ng/ml EGF + 20 ng/ml FGF). Cells are cultured either as a monolayer on Matrigel, or in suspension as neurospheres in T75 flasks. IMR90 fibroblasts were cultured in DMEM containing 10% fetal bovine serum (FBS) and grown to confluence prior to transplant.

To obtain a single cell suspension, cells were treated with Accutase for 5-10 min, pelleted and resuspended in a PBS solution containing 5 mM glucose and 0.1 mg/ml DNase at a concentration of 100,000 cells/μl.

Immunofluorescence (Cells)

After fixation with 4% paraformaldehyde for 20 minutes, the cells were incubated with 10% donkey serum for 1 hour, then incubated in primary antibodies overnight at 4ºC. After a PBS wash and incubation with secondary antibodies at RT for 2 hours, nuclei were counterstained with 4',6-diamidino-2-phenylindole (DAPI) and mounted.

Animals and Surgeries

Adult female Long-Evans rats were used in this study. Animals were 8 weeks old at initiation of training and approximately 5 months old at time of injury. Animals received intraperitoneal injections of 80 mg/kg ketamine and 15 mg/kg xylazine. A laminectomy was performed at the C4 spinous process of the lamina ipsilateral to the animal's dominant paw (determined via behavioral tasks described below).

The animals were then placed in a spinal frame and a contusion injury was conducted using a fourth generation Ohio State Injury Device (Horner and Stokes 1995). An electromagnetically controlled probe (0.7 mm end diameter, Ling Dynamics, Inc) was lowered to the surface of the cord just lateral to midline. The probe was oscillated on the surface of the spinal cord to achieve a common starting force of 3000 kilodynes for all animals. The spinal cord was displaced 0.8 mm for 14 msec to induce the injury. The surgical site was closed by suturing muscle in layers and closing skin with wound clips.

Four weeks after injury, scores on the forelimb reaching task (FRT, see below) stabilized, allowing for tight control for injury severity prior to transplantation. Thus, animals were assigned to treatment groups based on FRT such that all groups had equal average scores. All animals received transplants or control procedures at four weeks after injury. One group receiving hiPSC-NSCs (n=4) was followed for four weeks. The remaining animals were assigned to receive hiPSC-NSCs (n=11), IMR90 fibroblasts (n=11), PBS (n=11) or sham transplantation (n=11) and were followed for eight weeks.

In preparation for transplantation, animals were anesthetized and the injury site exposed. After placement in a spinal frame, a pulled glass capillary (OD 70-100 μm) was placed on the lateral border of the gray matter and stereotactically lowered to a depth of 1.0 mm, targeting the gray-white border of the dorsolateral funiculus. Animals in the hiPSC-NSC and fibroblast groups received two injections of 100,000 cells each (1.0 μl injected over 60 s), one rostral and one caudal to the injury site. The PBS group received two 1 μl injections, while sham animals were suspended in the frame but received no injection. Muscles were subsequently sutured in two

layers and the skin closed. All animals received daily subcutaneous injections of cyclosporine (10 mg/kg, Sandimmune) from the day of transplant to the time of sacrifice.

Tissue Processing

Animals were anesthetized and perfused transcardially with saline followed by 4% paraformaldehyde (PFA) in 0.1M phosphate buffer. Spinal columns were post-fixed overnight, cryoprotected with 30% sucrose, and then cut into five 1-mm coronal sections surrounding the lesion, embedded in OCT medium and flash frozen. 20 μm sections were cut on a Leica CM1850 cryostat in a one-in-six series and stored at -80ºC.

Immunofluorescence (Tissue)

Tissue was permeabilized with 0.4% Triton, then blocked with 5% donkey serum (DKS) and 0.4% Triton. Primary antibodies were applied to sections at 4˚C overnight. Slides were then rinsed 3 times in PBS, and incubated in the appropriate secondary antibody solution overnight at 4˚C. Sections were rinsed twice more with PBS, then incubated with DAPI before mounting.

To determine cell survival, stereology was conducted using a Zeiss Axioplan microscope and StereoInvestigator software (MBF Biosciences). Survival and proliferation of human cells was quantified by HuNu and Ki-67 immunolabeling with the optical disector probe and systematic random sampling according to stereological principles.

For quantification of hiPSC-NSC phenotypes *in vivo*, imaging of 15 sections per animal was performed on a Nikon Confocal microscope. A minimum of 100 HuNu+ cells per animal were counted, as were the numbers of human cells expressing doublecortin (Dcx), neuron-specific class III β-tubulin (TuJ1), oligodendrocyte transcription factor 2 (Olig2), glutathione S-

transferase pi (GSTpi), and human-specific glial fibrillary acidic protein (hGFAP), and percentages of HuNu-positive cells for each were calculated.

Antibodies

The following antibodies were used: Dcx (Santa Cruz, 1:100), GSTpi (Millipore, 1:500), hGFAP (StemCells, Inc., 1:1000), HoxB4 (Developmental Studies Hybridoma Bank, 1:100), HuNu (Millipore, 1:300), Ki-67 (Abcam, 1:500), Olig2 (Innovation Beyond Limits , 1:500), Sox1 (R&D Systems, 1:500), Sox9 (R&D Systems, 1:500), and TuJ1 (Covance, 1:1000).

Limb-Use Asymmetry Test

The limb-use asymmetry test (LUAT) was used to assess forelimb preference during vertical exploration in a clear Plexiglas cylinder. Animals were scored by blinded observers on independent and simultaneous use of their left and right forelimbs when rearing to make wall contacts (Schallert, Fleming et al. 2000; Gensel, Tovar et al. 2006). Each session lasted until an animal made 20 wall contacts. To determine the degree to which animals preferred their unaffected forelimb after injury, an asymmetry score was calculated for wall contacts for each test session, $asymmetry = [(affected\ forelimb) + .5(both\ forelimbs)]/20$, with a score below 0.5 indicating preference for the unaffected forelimb. No training is required for this test, and all animals prior to injury were close to a score of 0.5, indicating no paw preference.

Forelimb Reaching Task

The forelimb reaching task was used to assess skilled reaching ability (Alaverdashvili and Whishaw 2010). Animals were trained to extend their forelimb through a slot in a clear Plexiglas box to grasp and eat a chocolate-flavored 35 mg precision-ground food pellet (Bioserv).

In a series of 10-minute sessions, animals were first introduced to the food pellets and testing box, and gradually trained to reach through the slots to grasp pellets. Once animals showed a clear preference for reaching with either the left or right paw, the slot corresponding to the other paw was blocked off and animals were allowed to reach with only their preferred paw. Animals were trained until they were reaching consistently with a success rate ~70% (approximately 3 months training for all animals).

Throughout the experiment, animals were tested for 10 minutes or until they completed 20 trials. A trial was defined as any advance of the paw towards the pellet, concluding when the animal moved the pellet off of the indentation with its paw or left the front of the box. Experimenters blind to treatment groups recorded total successes, successes on the first attempt, and failures. A trial was considered successful when an animal grasped the pellet with the appropriate paw, transported it into the box, and placed it into its mouth without allowing the pellet to touch the floor.

Video Recording and Movement Analysis

Reaches during the FRT were video recorded with a Sony camcorder at a shutter speed of 1/1000 s. Individual elements of the reaches were identified via a conceptual framework derived from Eshkol-Wachmann Movement Notation (Whishaw and Pellis 1990; Alaverdashvili and Whishaw 2010) . The following movements were scored on the first three successful reaches of a session :

1. Orientation toward the pellet

2. Limb lift from the floor

3. Digit flexion

4. Aim

5. Advance of the forelimb through the slot

6. Digit extension

7. Pronation of the upper arm

8. Grasp of the pellet

9. Supination of the paw (I)

10. Supination of the paw (II)

11. Release of the pellet

12. Replacement of the paw on the floor

An observer blinded to treatment groups rated each element on a three-point scale: 0 = normal, 0.5 = present but abnormal, 1 = absent.

Statistical Analysis

Data presented are means ± SEM. Two-way ANOVA was performed on FRT and LUAT results. A paired two-tailed t-test was used to compare matched movement analysis scores before and after transplant within groups. An unpaired two-tailed t-test was used to compare phenotype data at 4 weeks and 15 weeks post-transplant.

Study Approval

All animal-related procedures were approved by the Institutional Animal Care and Use Committee of the University of Washington and were conducted in accordance with the guidelines of the NIH.

Results

Characterization of hiPSC-NSCs

IMR90 hiPSCs efficiently generated neural tube-like rosettes and expressed the neural stem cell markers Sox1 and Sox9 (Fig. 1a-c). hiPSC-NSCs could be further differentiated *in vivo* into GFAP+ astrocytes and TuJ1+ neurons (Fig. 1d-e). Telomerase activity was surveyed in hiPSC-NSCs and in undifferentiated hiPSC controls in order to assess retention of the capacity for unrestricted cell division after neuralization. Acitivity in hiPSC-NSCs (0.017 ± 0.002 amol/µg) was approximately 100-fold lower than in undifferentiated hiPSCs (1.503 ± 0.364 amol/µg), but slightly higher than that of heat-inactivated controls (0.000 ± 0.000 inactivated hiPSC-NSCs, 7.342e-008 ± 0.000 inactivated hiPSCs).

hiPSC-NSCs form neurons and glia in the chronically injured spinal cord 4 weeks after transplant

4 weeks after transplant, hiPSC-NSCs integrated into the injured spinal cord and were found exclusively ipsilateral to the contusion, primarily near the lesion cavity. 31.03 ± 13.01% of hiPSC-NSCs stained positively for the immature neuronal marker doublecortin (Dcx, Fig. 2a) (Brown, Couillard-Despres et al. 2003) and 25.23 ± 13.81% expressed TuJ1 (Fig. 2b), demonstrating the neurogenic capacity of hiPSC-NSCs in the spinal cord. Transplanted cells also formed GSTpi+ oligodendrocytes (22.83 ± 6.58%, Fig. 2c), and over half expressed the transcription factor Olig2 (55.75 ± 8.24%, Fig. 2d), a protein expressed by ventral neural progenitors and required for oligodendrocyte and motor neuron development. Relatively few (11.58 ± 3.265%) cells stained for a human-specific GFAP marker (hGFAP, Fig. 2e), indicating

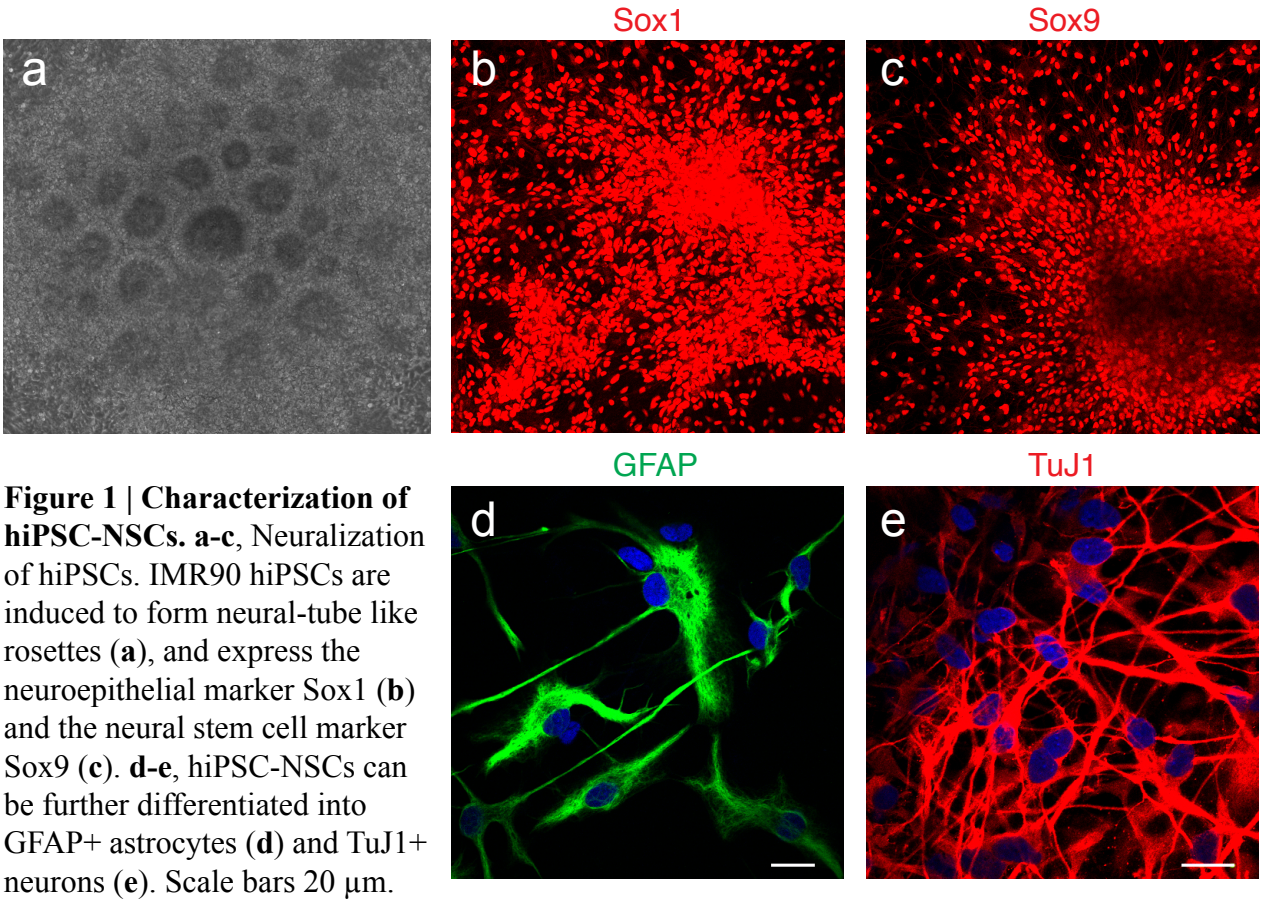

Figure 1 | Characterization of hiPSC-NSCs. a-c, Neuralization of hiPSCs. IMR90 hiPSCs are induced to form neural-tube like rosettes (**a**), and express the neuroepithelial marker Sox1 (**b**) and the neural stem cell marker Sox9 (**c**). **d-e**, hiPSC-NSCs can be further differentiated into GFAP+ astrocytes (**d**) and TuJ1+ neurons (**e**). Scale bars 20 μm. **f**, Compared to undifferentiated controls, hiPSC-NSCs exhibit very low levels of telomerase activity, as do heat-inactivated controls.

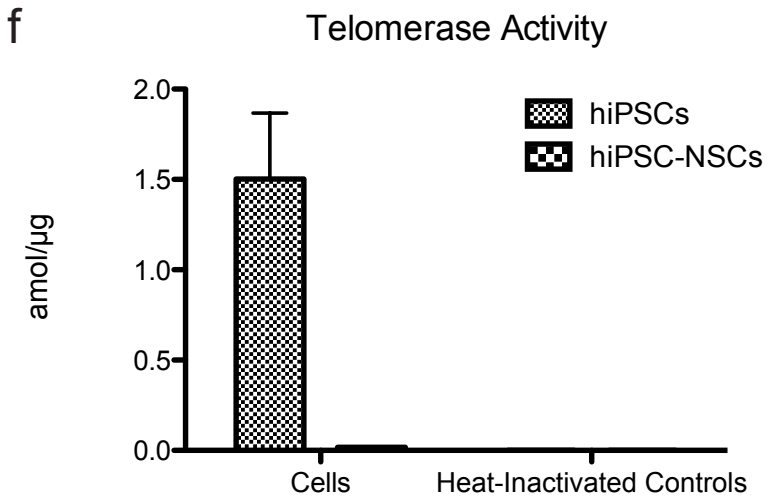

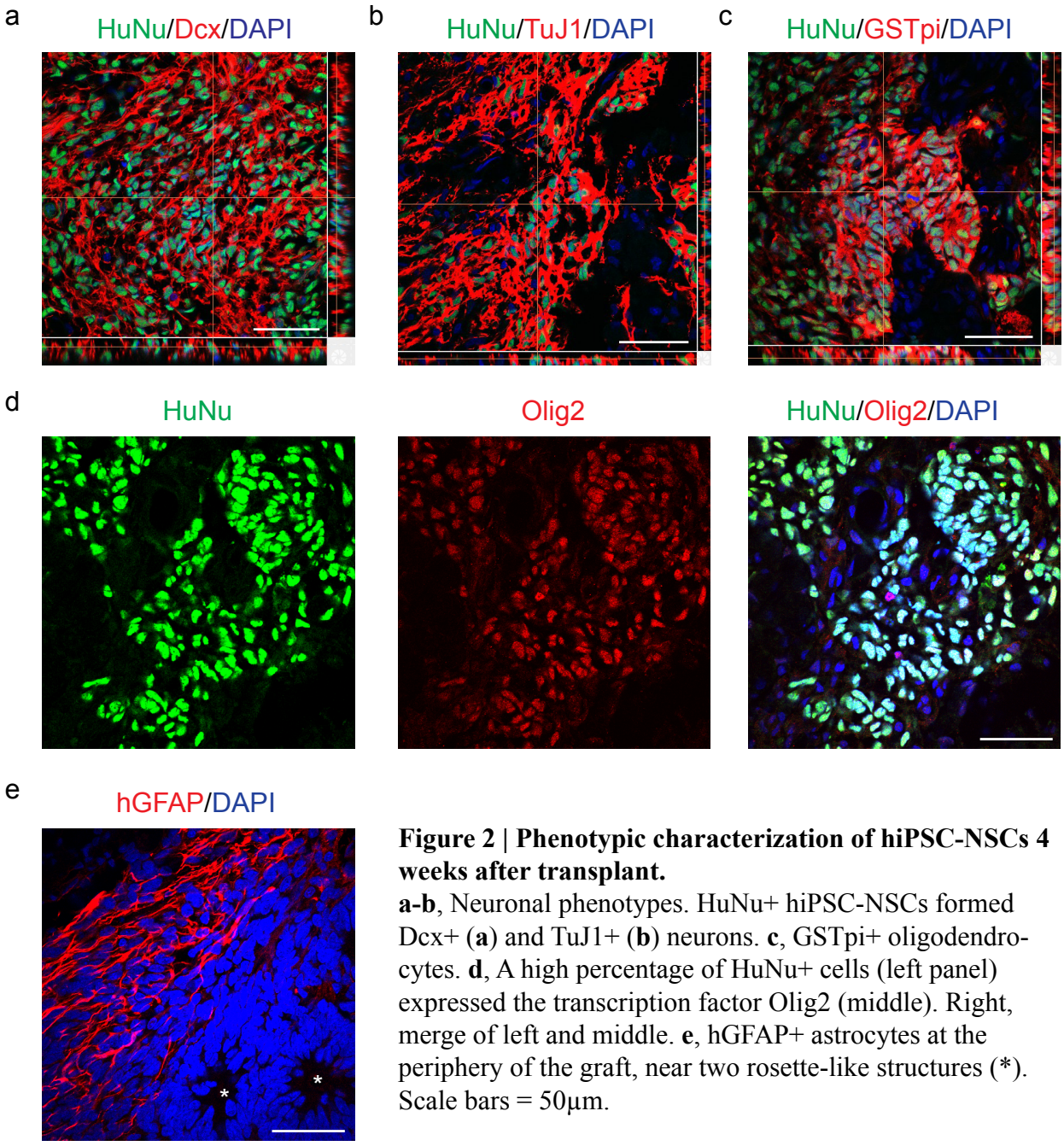

Figure 2 | Phenotypic characterization of hiPSC-NSCs 4 weeks after transplant.
a-b, Neuronal phenotypes. HuNu+ hiPSC-NSCs formed Dcx+ (**a**) and TuJ1+ (**b**) neurons. **c**, GSTpi+ oligodendrocytes. **d**, A high percentage of HuNu+ cells (left panel) expressed the transcription factor Olig2 (middle). Right, merge of left and middle. **e**, hGFAP+ astrocytes at the periphery of the graft, near two rosette-like structures (*). Scale bars = 50µm.

relatively few astrocytes at this stage. hiPSC-derived astrocytes tended to populate the periphery of the grafts at this time point.

Phenotypic changes in hiPSC-NSCs 15 weeks after transplant

15 weeks after transplant, hiPSC NSC-derived cells displayed a substantially different phenotypic profile than at 4 weeks. The percentage of Dcx+ immature neurons decreased to 8.891 ± 6.680% ($p = 0.0007$ compared to 4 weeks) (Fig. 3a) while the percentage of TuJ1+ neurons only slightly decreased to 19.68 ± 3.8% (Fig. 3b). Similar decreases were seen in percentages of Olig2 (12.68 ± 5.326%; $p < 0.0001$) and GSTpi (9.273 ± 5.474%; $p = 0.0118$). In contrast, there was a large increase in the percentage of hGFAP+ astrocytes (41.73 ± 7.723%; $p < 0.0001$).

Mitotic indices and rosettes decrease in number from 4 weeks to 15

4 weeks after transplant, 6.031 ± 2.850% of hiPSC-NSCs expressed the proliferation marker Ki-67 (Fig. 4a). Many neural rosette structures that resembled those observed *in vitro* were also present, with radially oriented columnar cells arranged around a central lumen. The rosettes detected were often surrounded by differentiated cells including neurons and glia (Fig. 2e). At 15 weeks, rosettes were not detected, and Ki-67 percentage was 3.834 ± 1.072%, lower than but not significantly different from the 4 week time point.

Behavioral analysis

Functional recovery was monitored via performance on two tasks: the skilled forelimb reaching task (FRT) and the unskilled limb-use asymmetry test (LUAT). At 8 and 9 weeks post-transplant, animals receiving hiPSC-NSCs tended to perform better than all 3 control groups (sham, fibroblast, PBS), though the difference was not statistically significant due to high variance (Fig.

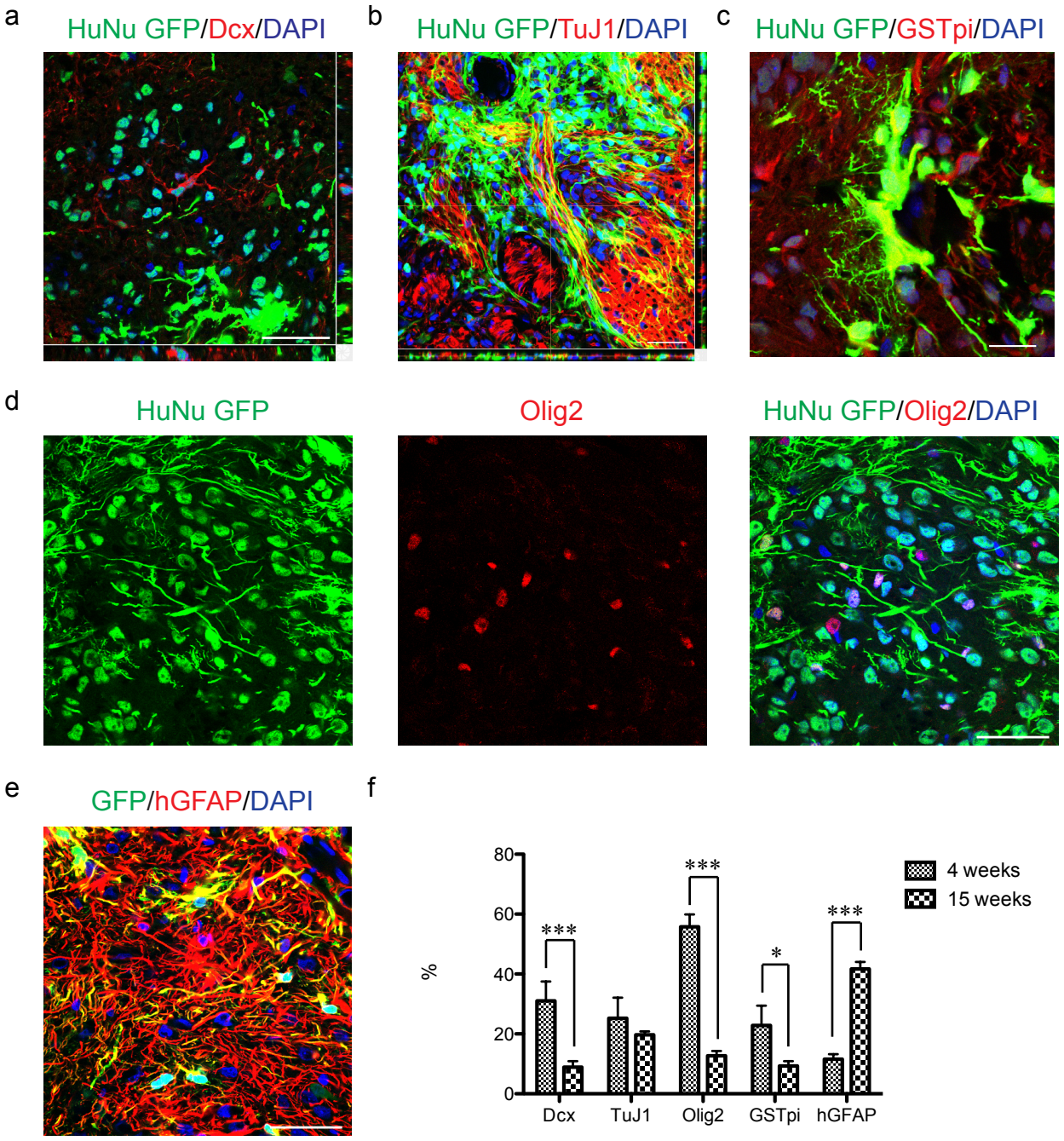

Figure 3 | Phenotypic characterization of hiPSC-NSCs 15 weeks after transplant.
a-b, Neuronal phenotypes. HuNu/GFP+ hiPSC-NSCs formed fewer Dcx+ (**a**) and more TuJ1+ (**b**) neurons compared to the 4 week time point. **c**, GFP+/GSTpi+ oligodendrocytes displayed complex morphologies. **d**, Some HuNu/GFP+ cells (left panel) retained Olig2 expression (middle). Right, merge of left and middle. **e**, hGFAP+ astrocytes. **f**, Quantification of markers at 4 and 15 weeks after transplant as a percentage of HuNu+ cells. Error bars are SEM.
* = $p < 0.05$; *** = $p < 0.001$. Scale bars = 50µm.

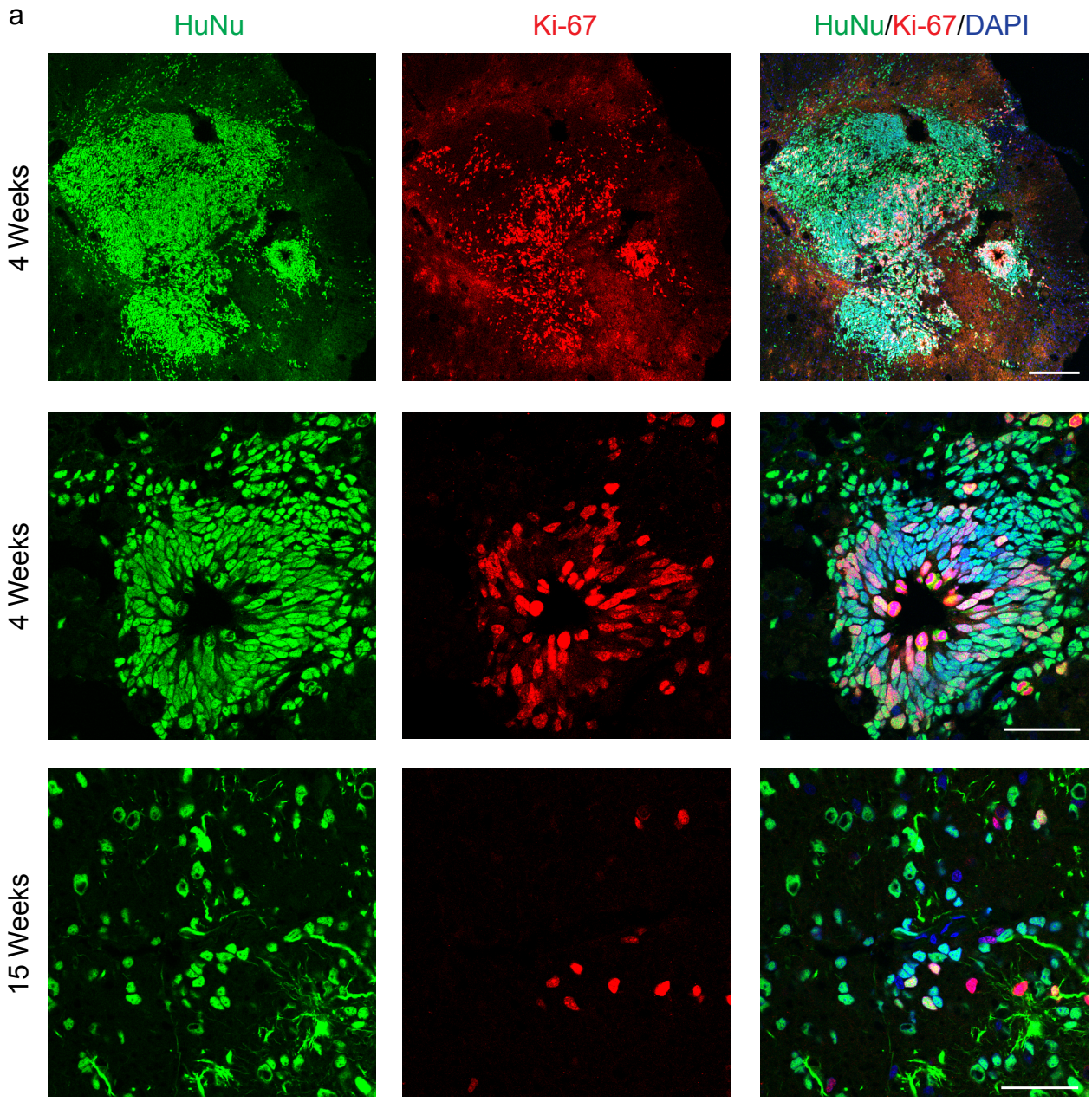

Figure 4 | Mitotic profile of hiPSC-NSCs. **a**, 4 weeks after transplant, 6.031% of hiPSC-NSCs were Ki-67+ (top two rows). At low (upper row) and high (middle row) magnification, radially oriented columnar cells in rosette-like structures were observed. 15 weeks after transplant (bottom row), Ki-67+ cells could still be detected. **b**, Quantification of Ki-67 as a percentage of HuNu+ cells. Error bars are SEM. Scale bars = 200 µm in top row, 50µm in middle and bottom.

5a). The trend was transient, as scores for the NSC group were comparable to controls by week 12 post-transplant and appeared to be declining over the last 3 weeks of the experiment.

On the LUAT, animals in all groups performed similarly at all time points and showed little improvement in paw preference over the course of the study (Fig. 5b). Scores of animals in the fibroblast group trended higher than other groups early after transplant. This was also transient, however, and comparisons across groups are not valid for the LUAT, as treatment assignments were based on FRT scores and LUAT scores varied across groups prior to transplant.

In order to more comprehensively assess recovery, rats were videotaped during the FRT and the videos scored on a rating system to evaluate reaching movements (Alaverdashvili, Leblond et al. 2008). Briefly, each reaching attempt was scored on 12 distinct movement elements, and each element was assigned a score of 0 (normal), 0.5 (present but abnormal) or 1 (absent). Prior to injury, animals in all groups achieved scores near or close to 0 on all elements (Fig. 6, left column). After injury, animals retained normal function in orientation and limb lifting, but displayed abnormal features of digit movement, aiming and paw advancement (Fig. 6, middle column). Elements of the reaching movement occurring after paw advancement (e.g. pronation, grasping, supination) were frequently absent. The profile of movement elements 15 weeks after transplant (Fig. 6, right column) was similar to that at 3 weeks after injury. No differences were observed between groups at a given time point, nor were significant differences observed within a group when comparing pre-transplant to post-transplant scores, with two exceptions. In the NSC group, scores on the “replace” element were significantly different ($p=0.0171$) when comparing pre-transplant to 15 weeks post-transplant scores. A significant difference was also detected making the same comparison for the sham group ($p=0.0183$).

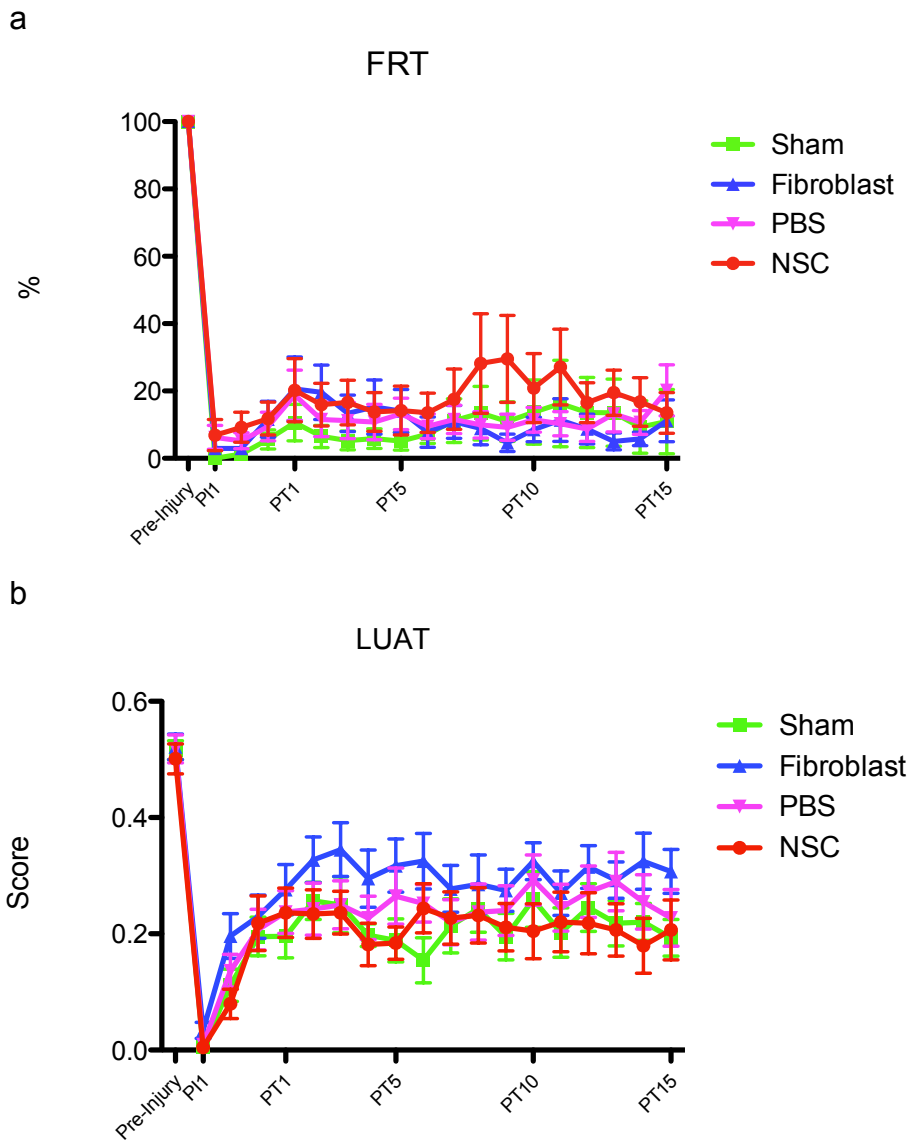

Figure 5 | Behavioral analysis: FRT and LUAT scores.
a, Forelimb reaching task performance. Animals that received hiPSC-NSCs trended toward performing better at weeks 8 and 9, but declined to scores comparable to controls by week 12. **b**, Limb-use asymmetry test performance. No differences were observed across groups at any time point. PIx indicates x weeks after injury, PTx x weeks after transplant. Error bars are SEM.

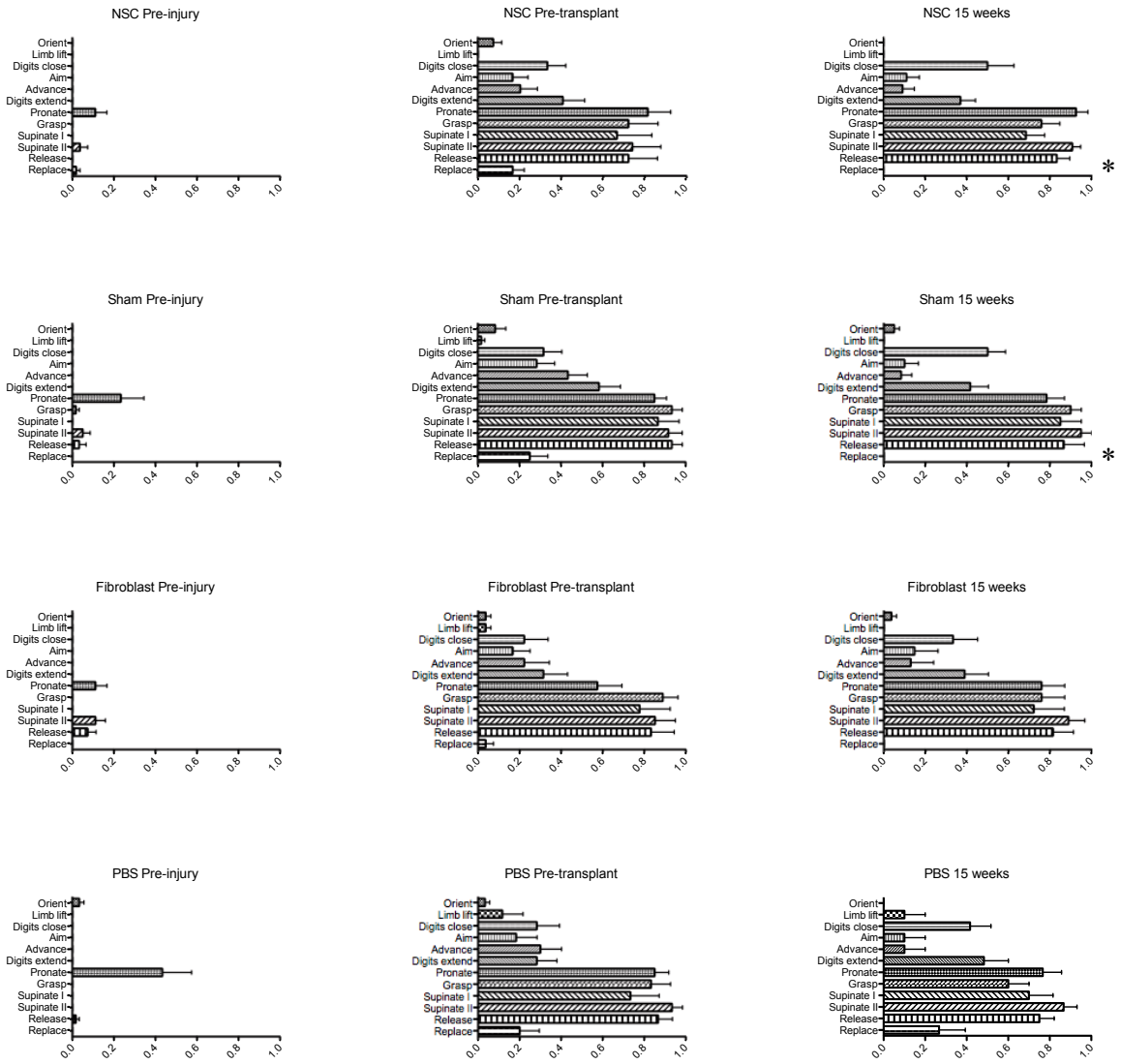

Figure 6 | Movement analysis. Movement element scores (mean ± SEM) before injury (left column), before transplant (middle column) and at the conclusion of the study (right column). Adult uninjured rats achieve scores close to 0. A score of 1 indicates absence of that element. * $p < 0.05$ compared to pre-transplant.

hiPSC-NSC overgrowth in vivo

On extraction of 4 out of the 11 cords in the 15 week post-transplant hiPSC-NSC group, discolored masses of vary sizes were observed (Fig. 7a). Hematoxylin and eosin stains revealed that the overgrowths were of heterogeneous cellularity, included neurons of various sizes and appeared to be encapsulated (Fig. 7b). Larger masses displaced the host tissue in the spinal cord far laterally (Fig. 7c), but did not appear to infiltrate the rat spinal cord. As demonstrated in Figure 3, the growths in all animals were composed primarily of neural elements, and did not have the histologic features of teratomas. Neural overgrowths did not contain rosette structures, but rather appeared to be largely disorganized, with the exception of bundles of TuJ1+ fibers in various regions. In addition to the 4 with obvious growths after extraction from the spinal column, 1 other animal had a large graft that appeared to be exerting some mass effect on histologic examination.

Discussion

While neural transplantation has proven effective in fostering cell replacement and locomotor recovery in acute and sub-acute time periods after SCI, chronic injury has proven more challenging. Here I reported the delivery of hiPSC-derived neural stem cells into highly clinically relevant model of spinal cord injury that involves the most commonly injured region (cervical) in the most prevalent temporal setting (chronic). hiPSC-NSCs proved effective at generating neurons and glia in the hostile lesion environment, retained neural phenotypes for 15 weeks after transplant and induced a trend in functional improvement on the forelimb reaching task. This trend did not reach statistical significance, however, and surprisingly dissipated by the

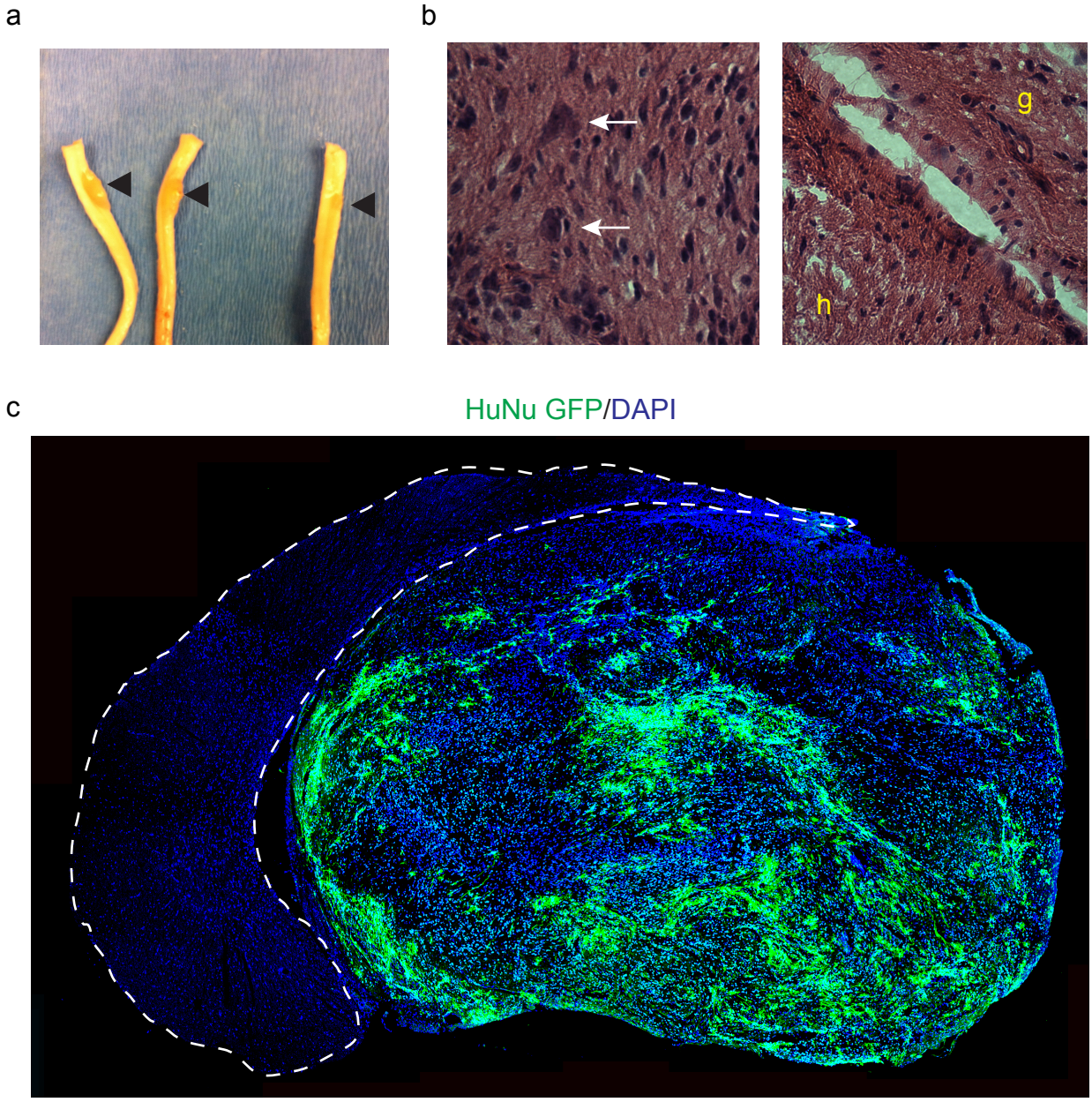

Figure 7 | hiPSC-NSC tumor growth after 15 weeks *in vivo*.
a, Photograph of three fixed spinal cords after extraction from the surrounding vertebrae. Discolored masses are indicated by black arrowheads. **b**, H&E stains. Left: two large neuronal nuclei (white arrows) with prominent nucleoli. Right: border between host tissue (h) and encapsulated graft (g). **c**, Cross-sectional image of tumor, showing lateral displacement of host tissue (outlined with dashed line).

conclusion of the experiment. Four out of 11 animals developed large intraparenchymal masses that were not teratomas, but rather comprised mostly of neural elements. This study calls attention to the need for rigorous safety measures in therapeutic hiPSC applications, beyond teratoma assays.

By four weeks after transplant into the injured spinal cord, hiPSC-NSCs had formed astrocytes, oligodendrocytes and neurons. A high percentage of the neurons detected were Dcx+, indicating an immature phenotype. This is in contrast to my previous work, where transplant of hiPSC-derived NPCs into the same model yielded very few Dcx+ cells after 4 weeks *in vivo*, and fewer at 8 weeks than hiPSC-NSCs generated at 4 weeks. The propensity for neurogenesis by hiPSC-NSCs relative to hiPSC-NPCs could have important implications in the design of cell replacement strategies for spinal cord injury and other CNS disorders. hiPSC-NSCs formed slightly lower proportions of GSTpi+ oligodendrocytes (9.273%) and hGFAP+ astrocytes (41.73%) at 15 weeks, than hiPSC-NPCs (17.2% GSTpi, 49.1% hGFAP) at 8 weeks. Future studies comparing the two cell populations could include both intermediate and longer time points to determine whether hiPSC-NPCs are inherently more disposed to gliogenesis or hiPSC-NSCs simply take longer to generate glia *in vivo* because they are less mature prior to transplant. The shift in phenotype by hiPSC-NSCs *in vivo* parallels several developmental principles. One is an apparent change in maturation from progenitors and precursors to more differentiated cells. 4 weeks after transplant, the most common markers detected are Olig2 and Dcx. Olig2 is a transcription factor found in ventral neural progenitors and their progeny (i.e. motor neurons and oligodendrocytes). It is probable that at 4 weeks, many Olig2+ cells are still in the progenitor phase given the high mitotic rate of cells, the lack of motor neuron morphologies and markers,

and that there were approximately only half as many GSTpi+ oligodendrocytes as Olig2+ cells. At 15 weeks, in contrast, the proportion of Olig2 decreased substantially, and was comparable to GSTpi, suggesting that most Olig2+ cells were oligodendrocytes at this point. It is also possible that the decline in Olig2 expression and increase in hGFAP are related, as loss or inactivation of Olig2 is essential to astrocyte differentiation (Gabay, Lowell et al. 2003; Fukuda, Kondo et al. 2004; Setoguchi and Kondo 2004). More rigorous analysis involving colocalization of Olig2 with progenitor, neuronal and oligodendrocyte markers is required before definitive statements can be made, however.

The proportionate decline in Dcx suggests a shift in maturation among neurons as well. Dcx is a microtubule-associated protein expressed by neuronal precursors and retained during early neuronal maturation (Brown, Couillard-Despres et al. 2003). While Dcx+ cells outnumbered TuJ1+ cells at 4 weeks, the reverse was true at 15 weeks. Additionally, the absolute percentage of Dcx declined over this time period. Taken together, these observations indicate a transition from immature neuronal phenotypes to fully differentiated neurons. If true, further analysis would be necessary to determine the phenotype (e.g. cholinergic, GABAergic) of these cells.

The preceding of gliogenesis by neurogenesis also mimics development. While neurons, especially immature ones, were prevalent at the early time point, astrocytes were not, though by 15 weeks they comprised nearly half the surviving cells. This time course closely parallels that of development *in vivo* (Liu and Zhang 2011), and of hiPSCs *in vitro* (Krencik, Weick et al. 2011). The studies described here are the first to my knowledge that demonstrate the late onset of gliogenesis by hiPSCs *in vivo*. During embryogenesis, fully functional oligodendrocytes don't appear until after neurons and astrocytes. This could account for the lack of myelin detected at

either time point (data not shown), despite the presence of GSTpi+ oligodendrocytes relatively early. Longer term experiments (perhaps up to a year) would help in determining whether additional time is all that is required for myelination by hiPSCs.

The presence of rosettes relatively early after transplant has been reported with hiPSC-NSCs in models of stroke (Jensen, Yan et al. 2011) and Parkinson's disease (Rhee, Ko et al. 2011). In the latter, cells proliferated extensively and occasionally caused tumor-related deaths. While I observed both rosettes and overgrowth of cells, no animals died or exhibited any visible effects such as excessive weight loss, though potential adverse outcomes associated with tumor formation were not monitored explicitly.

This study revealed several important points with regard to safety. First is that the tumors observed appeared to be encapsulated, were certainly well-demarcated, did not display features of teratomas and consisted mostly of neural cells. These findings demonstrate the need for expanding tumor surveillance beyond that necessary for teratomas (e.g. contamination of transplant material with undifferentiated cells). The precise identity of the tumors found here is as of yet undetermined. Given the multilineage but primarily neural nature of the cells involved, possible tumor classifications include primitive neuroectodermal tumors, malignant growths of varying degrees of differentiation (Becker and Hinton 1983), and dysembryoplastic neuroepithelial tumors, benign glial-neuronal tumors containing oligodendrocyte-like cells attached to axon bundles (Daumas-Duport, Scheithauer et al. 1988).

Additionally, my present and previous results underline the importance of stage of differentiation in evaluating safety and efficacy of transplanting pluripotent stem cells. hiPSCs differentiated to a neural progenitor state survive well and ultimately cease dividing in this model of spinal cord

injury, while those of a more immature neural stem cell phenotype (used in this study) had a propensity for overgrowth in some animals. Parkinson's disease research with both hESCs and hiPSCs have reported similar principles: immature neuralized cells carry a risk of tumor formation, intermediate progenitor/precursor cells graft well, and fully differentiated neurons show very poor survival (Rhee, Ko et al. 2011; Doi, Morizane et al. 2012). Tsuji et al showed that the difference between safe hiPSC-NSCs and unsafe, teratoma-inducing cells can be a single passage after neuralization (Tsuji, Miura et al. 2010). My results contradict this finding, as hiPSC-NSCs were passaged after neuralization and still retained tumorigenic capacity. The tumors observed in the present study were not teratomas, however, and there were many experimental differences such as differentiation protocol, injury model and hiPSC lines used. Still, the variation in safety results warrant further investigation into the specific principles that govern tumorigenic capacity in neuralized hiPSCs.

Conclusion

The broad differentiation potential of hiPSC-NSCs makes them an attractive resource for CNS regeneration, as these cells can effectively generate neurons and glia in the hostile chronic SCI environment, with modest effects on forelimb recovery. The associated risk of neural overgrowth calls attention to a new safety concern for hiPSC technology. While concerns about teratomas are well-founded with pluripotent stem cell transplantation, the scope of tumor surveillance should be expanded to include other classes of overgrowth. Only with the most stringent safety standards will hiPSCs achieve the clinical promise offered.

Chapter V: CONCLUSION

For my thesis, I evaluated the use of hiPSCs at three different differentiation states as potential therapeutic agents in chronic cervical spinal cord injury, a condition for which current treatment modalities are mostly ineffective. While driving hiPSCs to a fully differentiated state (i.e. astrocytes), with specific regional, morphological and phenotypic features, was feasible *in vitro*, hiPSC-derived astrocytes did not prove to be an effectively transplantable resource. Multipotent caudalized hiPSC-NPCs engrafted well into the hostile lesion environment and differentiated into multiple neural and glial cell types *in vivo* that translated into only modest functional recovery. Finally, transplantation of hiPSC-NSCs showed that broad differentiation potential brings a concomitant risk of overgrowth. Finding a balance between competency and unchecked proliferation will be key to effectively and safely realizing the potential of hiPSCs in spinal cord injury.

The first chapter demonstrated the ability of hiPSCs to form GFAP+ astrocytes across a spectrum of maturity. gp130 agonists (i.e. CNTF, CT-1) formed more immature astrocytes, as well as neurons. BMP-4, in contrast, formed more mature astrocytes with distinct morphologies and GLAST expression. Efforts to demonstrate synergy among astrocyte cues did not result in increased GFAP expression over single cytokines, but did suggest a dominance of BMP-4 over other cues in terms of morphologies and efficiency of astrocyte genesis. Whether hiPSC-generated astrocytes can achieve functional maturity remains to be seen, as GLAST expression alone is not a guarantee of glutamate buffering. Other functional astrocyte features yet to be demonstrated in hiPSC-derived cells include gap junction formation and calcium wave signaling.

hiPSC astrocytes did not survive well *in vivo* under the conditions tested here. It is possible that a greater number of cells is required, or that a different complement of factors is necessary in the transplant medium. Exogenous trophic support may also be effective in supporting cell survival. The inability of hiPSC-derived astrocytes to survive and integrate in the adult spinal cord does parallel findings with hiPSC-derived neurons. Future studies employing fetal or neonatal rats would assess whether the maturity of the host nervous system has an effect on relative engraftment success. It is also possible that astrocytes may, perhaps paradoxically, survive better in an injury environment.

The lack of success with differentiated cells encouraged us to try a less mature, multipotent cell type, i.e. hiPSC-NPCs. These cells had been generated via extensive patterning that conferred caudal region specificity and neurogenic and gliogenic capacity. When transplanted into the chronic cervical injury model, a high percentage of cells safely integrated and generated neurons, astrocytes and oligodendrocytes. Despite this, effects on functional recovery were minimal. It is probable that in the particularly challenging chronic injury environment, a combinatorial approach will be necessary to effect meaningful behavioral improvement that translates to enhanced quality of life. Other modalities to consider include trophic support, rehabilitation, and targeted reduction/ablation of the glial scar. The animals used in my studies did receive a form of rehabilitation by performing the forelimb reaching task 5 days a week, but this was not intended as an explicit rehabilitation program. A more directed approach would be better suited to assess the utility of rehabilitation.

I also conducted some pilot experiments combining chondroitinase ABC with hiPSC-NPCs or hiPSC-NSCs. Chondroitinase ABC digests chondroitin sulfate proteoglycans, extracellular

matrix molecules that are strongly inhibitory to nerve regeneration (Busch and Silver 2007). The inclusion of chondroitinase did not result in behavioral improvements in these small short-term (i.e. 4 weeks after transplant) experiments. As with rehabilitation, fully testing the therapeutic potential of chondroitinase with hiPSCs will require larger, carefully designed experiments.

Since hiPSC-NPCs were effective in generating neural cell types in the chronic contusion model, but did not significantly improve function on either skilled (FRT) or unskilled (LUAT) behavioral tests, I decided to employ less mature cells with presumably broader differentiation potential (hiPSC-NSCs) and observe animals for longer after transplant. While hiPSC-NSCs were also effective at generating neurons and glia *in vivo*, and even appeared to transiently improve behavior on the FRT at 8 and 9 weeks post-transplant, their potential for overgrowth proved too great to safely produce lasting benefits.

The modest and/or transient recoveries achieved with hiPSC-NSCs and hiPSC-NPCs are intriguing, but suggest the need for further optimization of these treatments in order to realize significant improvements. Further investigation into the mechanisms of the moderate effects observed so far will provide valuable information for enhancing the potential benefits of hiPSCs. For example, injection of hiPSC-NSC conditioned medium could be useful in determining whether hiPSC-NSCs exert effects primarily through the release of soluble factors, and would provide a means of avoiding neural overgrowth.

hiPSCs have the potential to provide plentiful autologous cells for clinical translation to spinal cord injury, but substantial hurdles remain. The necessary conditions for effective cell replacement and plasticity to occur in a safe manner are yet to be determined. In addition to the possible multifactorial approaches outlined above, it may be that combinations of cells will

demonstrate additive benefit and ultimately prove most effective. For despite the ability of a particular stem cell population to enhance a component of recovery, no single cell type tested thus far has proven sufficient to robustly restore function. Several groups have pursued combinations of Schwann cells with olfactory ensheathing cells or neural stem cells, demonstrating some synergy between the two populations in promoting anatomic plasticity and functional recovery (Fouad, Schnell et al. 2005; Guo, Zeng et al. 2007; Pearse, Sanchez et al. 2007). It may very well be that in order to fully harness the benefits of hiPSCs, multiple discrete populations will be required. The specific phenotypes selected will depend on the repair mechanisms targeted.

Cell-based therapies have demonstrated extensive potential for SCI, and there is considerable urgency felt by researchers to quickly translate these findings to the clinic. hiPSCs in particular seem ideally suited for clinical application as an abundant and autologous transplantable resource. However, as a consequence of being a new technology, hiPSC research has yielded relatively little data with regard to SCI. There is a need for solid preclinical foundation and demonstration of safety (both biological and procedural) before clinical trials can be attempted. Despite these caveats, hiPSC-derived neural cells still show promise as a means of inducing cellular plasticity in a vastly underserved population of patients suffering from chronic cervical SCI.

References

Adachi, K., H. Suemori, et al. (2010). "Role of SOX2 in maintaining pluripotency of human embryonic stem cells." Genes Cells **15**(5): 455-470.

Alaverdashvili, M., H. Leblond, et al. (2008). "Cineradiographic (video X-ray) analysis of skilled reaching in a single pellet reaching task provides insight into relative contribution of body, head, oral, and forelimb movement in rats." Behav Brain Res **192**(2): 232-247.

Alaverdashvili, M. and I. Q. Whishaw (2010). "Compensation aids skilled reaching in aging and in recovery from forelimb motor cortex stroke in the rat." Neuroscience **167**(1): 21-30.

Anderson, A. J., D. L. Haus, et al. (2011). "Achieving stable human stem cell engraftment and survival in the CNS: is the future of regenerative medicine immunodeficient?" Regen Med **6**(3): 367-406.

Anderson, D. K., M. Beattie, et al. (2005). "Recommended guidelines for studies of human subjects with spinal cord injury." Spinal Cord **43**(8): 453-458.

Anderson, K. D. (2004). "Targeting recovery: priorities of the spinal cord-injured population." J Neurotrauma **21**(10): 1371-1383.

Bachoo, R. M., R. S. Kim, et al. (2004). "Molecular diversity of astrocytes with implications for neurological disorders." Proc Natl Acad Sci U S A **101**(22): 8384-8389.

Bass, A. H. and R. Baker (1997). "Phenotypic specification of hindbrain rhombomeres and the origins of rhythmic circuits in vertebrates." Brain Behav Evol **50 Suppl 1**: 3-16.

Becker, L. E. and D. Hinton (1983). "Primitive neuroectodermal tumors of the central nervous system." Hum Pathol **14**(6): 538-550.

Bjorklund, L. M., R. Sanchez-Pernaute, et al. (2002). "Embryonic stem cells develop into functional dopaminergic neurons after transplantation in a Parkinson rat model." Proc Natl Acad Sci U S A **99**(4): 2344-2349.

Blight, A. R. (2002). "Miracles and molecules--progress in spinal cord repair." Nat Neurosci **5 Suppl**: 1051-1054.

Blomstrand, F., N. D. Aberg, et al. (1999). "Extent of intercellular calcium wave propagation is related to gap junction permeability and level of connexin-43 expression in astrocytes in primary cultures from four brain regions." Neuroscience **92**(1): 255-265.

Bradford, J., J. Y. Shin, et al. (2009). "Expression of mutant huntingtin in mouse brain astrocytes causes age-dependent neurological symptoms." Proc Natl Acad Sci U S A **106**(52): 22480-22485.

Brennand, K. J., A. Simone, et al. (2011). "Modelling schizophrenia using human induced pluripotent stem cells." Nature **473**(7346): 221-225.

Brenner, M., A. B. Johnson, et al. (2001). "Mutations in GFAP, encoding glial fibrillary acidic protein, are associated with Alexander disease." Nat Genet **27**(1): 117-120.

Brimble, S. N., X. Zeng, et al. (2004). "Karyotypic stability, genotyping, differentiation, feeder-free maintenance, and gene expression sampling in three human embryonic stem cell lines derived prior to August 9, 2001." Stem Cells Dev **13**(6): 585-597.

Brown, J. P., S. Couillard-Despres, et al. (2003). "Transient expression of doublecortin during adult neurogenesis." J Comp Neurol **467**(1): 1-10.

Busch, S. A. and J. Silver (2007). "The role of extracellular matrix in CNS regeneration." Curr Opin Neurobiol **17**(1): 120-127.

CDRF. (2009, 2009). "Prevalence of Paralysis." Retrieved May 17, 2012, from http://www.christopherreeve.org/site/c.mtKZKgMWKwG/b.5184255/k.6D74/Prevalence_of_Paralysis.htm.

Chambers, S. M., C. A. Fasano, et al. (2009). "Highly efficient neural conversion of human ES and iPS cells by dual inhibition of SMAD signaling." Nat Biotechnol **27**(3): 275-280.

Cheng, L. C., E. Pastrana, et al. (2009). "miR-124 regulates adult neurogenesis in the subventricular zone stem cell niche." Nat Neurosci **12**(4): 399-408.

Chong, S. Y. and J. R. Chan (2010). "Tapping into the glial reservoir: cells committed to remaining uncommitted." J Cell Biol **188**(3): 305-312.

Cummings, B. J., N. Uchida, et al. (2005). "Human neural stem cells differentiate and promote locomotor recovery in spinal cord-injured mice." Proc Natl Acad Sci U S A **102**(39): 14069-14074.

D'Alessandro, J. S. and E. A. Wang (1994). "Bone morphogenetic proteins inhibit proliferation, induce reversible differentiation and prevent cell death in astrocyte lineage cells." Growth Factors **11**(1): 45-52.

Daumas-Duport, C., B. W. Scheithauer, et al. (1988). "Dysembryoplastic neuroepithelial tumor: a surgically curable tumor of young patients with intractable partial seizures. Report of thirty-nine cases." Neurosurgery **23**(5): 545-556.

David, S. and A. J. Aguayo (1981). "Axonal elongation into peripheral nervous system "bridges" after central nervous system injury in adult rats." Science **214**(4523): 931-933.

Davies, J. E., C. Proschel, et al. (2008). "Transplanted astrocytes derived from BMP- or CNTF-treated glial-restricted precursors have opposite effects on recovery and allodynia after spinal cord injury." J Biol **7**(7): 24.

Davies, S. J., C. H. Shih, et al. (2011). "Transplantation of specific human astrocytes promotes functional recovery after spinal cord injury." PLoS One **6**(3): e17328.

de Leon, R. D., H. Tamaki, et al. (1999). "Hindlimb locomotor and postural training modulates glycinergic inhibition in the spinal cord of the adult spinal cat." J Neurophysiol **82**(1): 359-369.

Dimos, J. T., K. T. Rodolfa, et al. (2008). "Induced pluripotent stem cells generated from patients with ALS can be differentiated into motor neurons." Science **321**(5893): 1218-1221.

Doetsch, F. (2003). "The glial identity of neural stem cells." Nat Neurosci **6**(11): 1127-1134.

Doi, D., A. Morizane, et al. (2012). "Prolonged maturation culture favors a reduction in the tumorigenicity and the dopaminergic function of human ESC-derived neural cells in a primate model of Parkinson's disease." Stem Cells **30**(5): 935-945.

Drejer, J., O. M. Larsson, et al. (1982). "Characterization of L-glutamate uptake into and release from astrocytes and neurons cultured from different brain regions." Exp Brain Res **47**(2): 259-269.

Dyer, C. A. and J. A. Benjamins (1989). "Organization of oligodendroglial membrane sheets: II. Galactocerebroside:antibody interactions signal changes in cytoskeleton and myelin basic protein." J Neurosci Res **24**(2): 212-221.

Dyer, C. A. and J. A. Benjamins (1989). "Organization of oligodendroglial membrane sheets. I: Association of myelin basic protein and 2',3'-cyclic nucleotide 3'-phosphohydrolase with cytoskeleton." J Neurosci Res **24**(2): 201-211.

Ebert, A. D., J. Yu, et al. (2009). "Induced pluripotent stem cells from a spinal muscular atrophy patient." Nature **457**(7227): 277-280.

Ellis, P., B. M. Fagan, et al. (2004). "SOX2, a persistent marker for multipotential neural stem cells derived from embryonic stem cells, the embryo or the adult." Dev Neurosci **26**(2-4): 148-165.

Emsley, J. G. and T. Hagg (2003). "Endogenous and exogenous ciliary neurotrophic factor enhances forebrain neurogenesis in adult mice." Exp Neurol **183**(2): 298-310.

Emsley, J. G. and J. D. Macklis (2006). "Astroglial heterogeneity closely reflects the neuronal-defined anatomy of the adult murine CNS." Neuron Glia Biol **2**(3): 175-186.

Erdo, F., C. Buhrle, et al. (2003). "Host-dependent tumorigenesis of embryonic stem cell transplantation in experimental stroke." J Cereb Blood Flow Metab **23**(7): 780-785.

Fawcett, J. W., A. Curt, et al. (2007). "Guidelines for the conduct of clinical trials for spinal cord injury as developed by the ICCP panel: spontaneous recovery after spinal cord injury and statistical power needed for therapeutic clinical trials." Spinal Cord **45**(3): 190-205.

Fehlings, M. G. and R. Vawda (2011). "Cellular treatments for spinal cord injury: the time is right for clinical trials." Neurotherapeutics **8**(4): 704-720.

Filbin, M. T. (2003). "Myelin-associated inhibitors of axonal regeneration in the adult mammalian CNS." Nat Rev Neurosci **4**(9): 703-713.

Filous, A. R., J. H. Miller, et al. (2010). "Immature astrocytes promote CNS axonal regeneration when combined with chondroitinase ABC." Dev Neurobiol **70**(12): 826-841.

Fouad, K., L. Schnell, et al. (2005). "Combining Schwann cell bridges and olfactory-ensheathing glia grafts with chondroitinase promotes locomotor recovery after complete transection of the spinal cord." J Neurosci **25**(5): 1169-1178.

Franceschini, M., B. Di Clemente, et al. (2003). "Longitudinal outcome 6 years after spinal cord injury." Spinal Cord **41**(5): 280-285.

Fujimoto, Y., M. Abematsu, et al. (2012). "Treatment of a Mouse Model of Spinal Cord Injury by Transplantation of Human iPS Cell-derived Long-term Self-renewing Neuroepithelial-like Stem Cells." Stem Cells.

Fukuda, S., T. Kondo, et al. (2004). "Negative regulatory effect of an oligodendrocytic bHLH factor OLIG2 on the astrocytic differentiation pathway." Cell Death Differ **11**(2): 196-202.

Gabay, L., S. Lowell, et al. (2003). "Deregulation of dorsoventral patterning by FGF confers trilineage differentiation capacity on CNS stem cells in vitro." Neuron **40**(3): 485-499.

Geller, H. M. and J. W. Fawcett (2002). "Building a bridge: engineering spinal cord repair." Exp Neurol **174**(2): 125-136.

Gensel, J. C., C. A. Tovar, et al. (2006). "Behavioral and histological characterization of unilateral cervical spinal cord contusion injury in rats." J Neurotrauma **23**(1): 36-54.

Guatteo, E., K. A. Stanness, et al. (1996). "Hyperpolarization-activated ion currents in cultured rat cortical and spinal cord astrocytes." Glia **16**(3): 196-209.

Guo, J. S., Y. S. Zeng, et al. (2007). "Cotransplant of neural stem cells and NT-3 gene modified Schwann cells promote the recovery of transected spinal cord injury." Spinal Cord **45**(1): 15-24.

Haas, C., B. Neuhuber, et al. (2012). "Phenotypic analysis of astrocytes derived from glial restricted precursors and their impact on axon regeneration." Exp Neurol **233**(2): 717-732.

Halassa, M. M., T. Fellin, et al. (2007). "Synaptic islands defined by the territory of a single astrocyte." J Neurosci **27**(24): 6473-6477.

Hedlund, E., J. Pruszak, et al. (2007). "Selection of embryonic stem cell-derived enhanced green fluorescent protein-positive dopamine neurons using the tyrosine hydroxylase promoter is confounded by reporter gene expression in immature cell populations." Stem Cells **25**(5): 1126-1135.

Hewett, J. A. (2009). "Determinants of regional and local diversity within the astroglial lineage of the normal central nervous system." J Neurochem **110**(6): 1717-1736.

Hofstetter, C. P., N. A. Holmstrom, et al. (2005). "Allodynia limits the usefulness of intraspinal neural stem cell grafts; directed differentiation improves outcome." Nat Neurosci **8**(3): 346-353.

Hofstetter, C. P., E. J. Schwarz, et al. (2002). "Marrow stromal cells form guiding strands in the injured spinal cord and promote recovery." Proc Natl Acad Sci U S A **99**(4): 2199-2204.

Horner, P. J. and B. T. Stokes (1995). "Fetal transplantation following spinal contusion injury results in chronic alterations in CNS glucose metabolism." Exp Neurol **133**(2): 231-243.

Houle, J. D. and A. Tessler (2003). "Repair of chronic spinal cord injury." Exp Neurol **182**(2): 247-260.

Hu, B. Y., Z. W. Du, et al. (2009). "Human oligodendrocytes from embryonic stem cells: conserved SHH signaling networks and divergent FGF effects." Development **136**(9): 1443-1452.

Hu, B. Y., Z. W. Du, et al. (2009). "Differentiation of human oligodendrocytes from pluripotent stem cells." Nat Protoc **4**(11): 1614-1622.

Hu, B. Y., J. P. Weick, et al. (2010). "Neural differentiation of human induced pluripotent stem cells follows developmental principles but with variable potency." Proc Natl Acad Sci U S A **107**(9): 4335-4340.

Hu, B. Y. and S. C. Zhang (2009). "Differentiation of spinal motor neurons from pluripotent human stem cells." Nat Protoc **4**(9): 1295-1304.

Hulsebosch, C. E. (2002). "Recent advances in pathophysiology and treatment of spinal cord injury." Adv Physiol Educ **26**(1-4): 238-255.

Iadecola, C. and M. Nedergaard (2007). "Glial regulation of the cerebral microvasculature." Nat Neurosci **10**(11): 1369-1376.

Ikegami, T., M. Nakamura, et al. (2005). "Chondroitinase ABC combined with neural stem/progenitor cell transplantation enhances graft cell migration and outgrowth of growth-associated protein-43-positive fibers after rat spinal cord injury." Eur J Neurosci **22**(12): 3036-3046.

Israel, J. M., C. G. Schipke, et al. (2003). "GABAA receptor-expressing astrocytes in the supraoptic nucleus lack glutamate uptake and receptor currents." Glia **44**(2): 102-110.

Israel, M. A., S. H. Yuan, et al. (2012). "Probing sporadic and familial Alzheimer's disease using induced pluripotent stem cells." Nature **482**(7384): 216-220.

Iwanami, A., S. Kaneko, et al. (2005). "Transplantation of human neural stem cells for spinal cord injury in primates." J Neurosci Res **80**(2): 182-190.

Jacob, J., A. Hacker, et al. (2001). "Mechanisms and molecules in motor neuron specification and axon pathfinding." Bioessays **23**(7): 582-595.

Jensen, M. B., H. Yan, et al. (2011). "Survival and Differentiation of Transplanted Neural Stem Cells Derived from Human Induced Pluripotent Stem Cells in A Rat Stroke Model." J Stroke Cerebrovasc Dis.

Johe, K. K., T. G. Hazel, et al. (1996). "Single factors direct the differentiation of stem cells from the fetal and adult central nervous system." Genes Dev **10**(24): 3129-3140.

Johnson, M. A., J. P. Weick, et al. (2007). "Functional neural development from human embryonic stem cells: accelerated synaptic activity via astrocyte coculture." J Neurosci **27**(12): 3069-3077.

Kang, P., H. K. Lee, et al. (2012). "Sox9 and NFIA Coordinate a Transcriptional Regulatory Cascade during the Initiation of Gliogenesis." Neuron **74**(1): 79-94.

Karimi-Abdolrezaee, S., E. Eftekharpour, et al. (2010). "Synergistic effects of transplanted adult neural stem/progenitor cells, chondroitinase, and growth factors promote functional repair and plasticity of the chronically injured spinal cord." J Neurosci **30**(5): 1657-1676.

Keirstead, H. S., G. Nistor, et al. (2005). "Human embryonic stem cell-derived oligodendrocyte progenitor cell transplants remyelinate and restore locomotion after spinal cord injury." J Neurosci **25**(19): 4694-4705.

Krencik, R., J. P. Weick, et al. (2011). "Specification of transplantable astroglial subtypes from human pluripotent stem cells." Nat Biotechnol **29**(6): 528-534.

Kumagai, G., Y. Okada, et al. (2009). "Roles of ES cell-derived gliogenic neural stem/progenitor cells in functional recovery after spinal cord injury." PLoS One **4**(11): e7706.

Kwon, B. K., J. Hillyer, et al. (2010). "Translational research in spinal cord injury: a survey of opinion from the SCI community." J Neurotrauma **27**(1): 21-33.

Kwon, B. K., J. Liu, et al. (2002). "Survival and regeneration of rubrospinal neurons 1 year after spinal cord injury." Proc Natl Acad Sci U S A **99**(5): 3246-3251.

Kwon, B. K., T. R. Oxland, et al. (2002). "Animal models used in spinal cord regeneration research." Spine (Phila Pa 1976) **27**(14): 1504-1510.

Lee, S. H., W. T. Kim, et al. (1994). "Astrocytes exhibit regional specificity in gap-junction coupling." Glia **11**(4): 315-325.

Lepore, A. C., B. Rauck, et al. (2008). "Focal transplantation-based astrocyte replacement is neuroprotective in a model of motor neuron disease." Nat Neurosci **11**(11): 1294-1301.

Li, X. J., Z. W. Du, et al. (2005). "Specification of motoneurons from human embryonic stem cells." Nat Biotechnol **23**(2): 215-221.

Liu, H. and S. C. Zhang (2011). "Specification of neuronal and glial subtypes from human pluripotent stem cells." Cell Mol Life Sci **68**(24): 3995-4008.

Maherali, N., R. Sridharan, et al. (2007). "Directly reprogrammed fibroblasts show global epigenetic remodeling and widespread tissue contribution." Cell Stem Cell **1**(1): 55-70.

Matyash, V. and H. Kettenmann (2010). "Heterogeneity in astrocyte morphology and physiology." Brain Res Rev **63**(1-2): 2-10.

Mitsui, T., J. S. Shumsky, et al. (2005). "Transplantation of neuronal and glial restricted precursors into contused spinal cord improves bladder and motor functions, decreases thermal hypersensitivity, and modifies intraspinal circuitry." J Neurosci **25**(42): 9624-9636.

Miura, K., Y. Okada, et al. (2009). "Variation in the safety of induced pluripotent stem cell lines." Nat Biotechnol **27**(8): 743-745.

Molofsky, A. V., R. Krenick, et al. (2012). "Astrocytes and disease: a neurodevelopmental perspective." Genes Dev **26**(9): 891-907.

Mulcahey, M. J., B. T. Smith, et al. (1994). "Functional neuromuscular stimulation: outcomes in young people with tetraplegia." J Am Paraplegia Soc **17**(1): 20-35.

Nagai, M., D. B. Re, et al. (2007). "Astrocytes expressing ALS-linked mutated SOD1 release factors selectively toxic to motor neurons." Nat Neurosci **10**(5): 615-622.

Nakashima, K., M. Yanagisawa, et al. (1999). "Synergistic signaling in fetal brain by STAT3-Smad1 complex bridged by p300." Science **284**(5413): 479-482.

Nakashima, K., M. Yanagisawa, et al. (1999). "Astrocyte differentiation mediated by LIF in cooperation with BMP2." FEBS Lett **457**(1): 43-46.

Nash, M. S. (2000). "Known and plausible modulators of depressed immune functions following spinal cord injuries." J Spinal Cord Med **23**(2): 111-120.

National Spinal Cord Injury Statistical Center, B., Alabama. (2011). "Spinal Cord Injury Facts and Figures at a Glance." Retrieved May 17, 2012, from www.nscisc.uab.edu.

Nori, S., Y. Okada, et al. (2011). "Grafted human-induced pluripotent stem-cell-derived neurospheres promote motor functional recovery after spinal cord injury in mice." Proc Natl Acad Sci U S A **108**(40): 16825-16830.

Nornes, H., A. Bjorklund, et al. (1983). "Reinnervation of the denervated adult spinal cord of rats by intraspinal transplants of embryonic brain stem neurons." Cell Tissue Res **230**(1): 15-35.

Oberheim, N. A., G. F. Tian, et al. (2008). "Loss of astrocytic domain organization in the epileptic brain." J Neurosci **28**(13): 3264-3276.

Ochiai, W., M. Yanagisawa, et al. (2001). "Astrocyte differentiation of fetal neuroepithelial cells involving cardiotrophin-1-induced activation of STAT3." Cytokine **14**(5): 264-271.

Ogawa, Y., K. Sawamoto, et al. (2002). "Transplantation of in vitro-expanded fetal neural progenitor cells results in neurogenesis and functional recovery after spinal cord contusion injury in adult rats." J Neurosci Res **69**(6): 925-933.

Okada, S., K. Ishii, et al. (2005). "In vivo imaging of engrafted neural stem cells: its application in evaluating the optimal timing of transplantation for spinal cord injury." FASEB J **19**(13): 1839-1841.

Oki, K., J. Tatarishvili, et al. (2012). "Human-Induced Pluripotent Stem Cells form Functional Neurons and Improve Recovery After Grafting in Stroke-Damaged Brain." Stem Cells **30**(6): 1120-1133.

Pallini, R., E. Fernandez, et al. (1988). "Retrograde degeneration of corticospinal axons following transection of the spinal cord in rats. A quantitative study with anterogradely transported horseradish peroxidase." J Neurosurg **68**(1): 124-128.

Pankratz, M. T., X. J. Li, et al. (2007). "Directed neural differentiation of human embryonic stem cells via an obligated primitive anterior stage." Stem Cells **25**(6): 1511-1520.

Park, I. H., N. Arora, et al. (2008). "Disease-specific induced pluripotent stem cells." Cell **134**(5): 877-886.

Pearse, D. D., A. R. Sanchez, et al. (2007). "Transplantation of Schwann cells and/or olfactory ensheathing glia into the contused spinal cord: Survival, migration, axon association, and functional recovery." Glia **55**(9): 976-1000.

Pfeifer, K., M. Vroemen, et al. (2004). "Adult neural progenitor cells provide a permissive guiding substrate for corticospinal axon growth following spinal cord injury." Eur J Neurosci **20**(7): 1695-1704.

Powers, B. E., J. Lasiene, et al. (2012). "Axonal Thinning and Extensive Remyelination without Chronic Demyelination in Spinal Injured Rats." J Neurosci **32**(15): 5120-5125.

Pruszak, J., K. C. Sonntag, et al. (2007). "Markers and methods for cell sorting of human embryonic stem cell-derived neural cell populations." Stem Cells **25**(9): 2257-2268.

Rhee, Y. H., J. Y. Ko, et al. (2011). "Protein-based human iPS cells efficiently generate functional dopamine neurons and can treat a rat model of Parkinson disease." J Clin Invest **121**(6): 2326-2335.

Robel, S., B. Berninger, et al. (2011). "The stem cell potential of glia: lessons from reactive gliosis." Nat Rev Neurosci **12**(2): 88-104.

Ross, S. E., M. E. Greenberg, et al. (2003). "Basic helix-loop-helix factors in cortical development." Neuron **39**(1): 13-25.

Rouach, N., A. Koulakoff, et al. (2008). "Astroglial metabolic networks sustain hippocampal synaptic transmission." Science **322**(5907): 1551-1555.

Rowitch, D. H. and A. R. Kriegstein (2010). "Developmental genetics of vertebrate glial-cell specification." Nature **468**(7321): 214-222.

Roy, N. S., C. Cleren, et al. (2006). "Functional engraftment of human ES cell-derived dopaminergic neurons enriched by coculture with telomerase-immortalized midbrain astrocytes." Nat Med **12**(11): 1259-1268.

Salazar, D. L., N. Uchida, et al. (2010). "Human neural stem cells differentiate and promote locomotor recovery in an early chronic spinal cord injury NOD-scid mouse model." PLoS One **5**(8): e12272.

Schallert, T., S. M. Fleming, et al. (2000). "CNS plasticity and assessment of forelimb sensorimotor outcome in unilateral rat models of stroke, cortical ablation, parkinsonism and spinal cord injury." Neuropharmacology **39**(5): 777-787.

Scholzen, T. and J. Gerdes (2000). "The Ki-67 protein: from the known and the unknown." J Cell Physiol **182**(3): 311-322.

Schwab, M. E. and D. Bartholdi (1996). "Degeneration and regeneration of axons in the lesioned spinal cord." Physiol Rev **76**(2): 319-370.

Scott, C. E., S. L. Wynn, et al. (2010). "SOX9 induces and maintains neural stem cells." Nat Neurosci **13**(10): 1181-1189.

Sekhon, L. H. and M. G. Fehlings (2001). "Epidemiology, demographics, and pathophysiology of acute spinal cord injury." Spine (Phila Pa 1976) **26**(24 Suppl): S2-12.

Setoguchi, T. and T. Kondo (2004). "Nuclear export of OLIG2 in neural stem cells is essential for ciliary neurotrophic factor-induced astrocyte differentiation." J Cell Biol **166**(7): 963-968.

Smith, G. M. and R. H. Miller (1991). "Immature type-1 astrocytes suppress glial scar formation, are motile and interact with blood vessels." Brain Res **543**(1): 111-122.

Smith, G. M., R. H. Miller, et al. (1987). "Astrocyte transplantation induces callosal regeneration in postnatal acallosal mice." Ann N Y Acad Sci **495**: 185-206.

Smith, G. M., U. Rutishauser, et al. (1990). "Maturation of astrocytes in vitro alters the extent and molecular basis of neurite outgrowth." Dev Biol **138**(2): 377-390.

Sofroniew, M. V. (2009). "Molecular dissection of reactive astrogliosis and glial scar formation." Trends Neurosci **32**(12): 638-647.

Soldner, F., D. Hockemeyer, et al. (2009). "Parkinson's disease patient-derived induced pluripotent stem cells free of viral reprogramming factors." Cell **136**(5): 964-977.

Stolt, C. C., P. Lommes, et al. (2003). "The Sox9 transcription factor determines glial fate choice in the developing spinal cord." Genes Dev **17**(13): 1677-1689.

Suhr, S. T., E. A. Chang, et al. (2009). "Telomere dynamics in human cells reprogrammed to pluripotency." PLoS One **4**(12): e8124.

Takahashi, K., K. Tanabe, et al. (2007). "Induction of pluripotent stem cells from adult human fibroblasts by defined factors." Cell **131**(5): 861-872.

Tator, C. H. and M. G. Fehlings (1991). "Review of the secondary injury theory of acute spinal cord trauma with emphasis on vascular mechanisms." J Neurosurg **75**(1): 15-26.

Tebar, L. A., S. M. Geranton, et al. (2008). "Deletion of the mouse RegIIIbeta (Reg2) gene disrupts ciliary neurotrophic factor signaling and delays myelination of mouse cranial motor neurons." Proc Natl Acad Sci U S A **105**(32): 11400-11405.

Teng, Y. D., E. B. Lavik, et al. (2002). "Functional recovery following traumatic spinal cord injury mediated by a unique polymer scaffold seeded with neural stem cells." Proc Natl Acad Sci U S A **99**(5): 3024-3029.

Teng, Y. D., W. L. Liao, et al. (2006). "Physical activity-mediated functional recovery after spinal cord injury: potential roles of neural stem cells." Regen Med **1**(6): 763-776.

Tetzlaff, W., E. B. Okon, et al. (2011). "A systematic review of cellular transplantation therapies for spinal cord injury." J Neurotrauma **28**(8): 1611-1682.

Thomson, J. A. and V. S. Marshall (1998). "Primate embryonic stem cells." Curr Top Dev Biol **38**: 133-165.

Tillakaratne, N. J., R. D. de Leon, et al. (2002). "Use-dependent modulation of inhibitory capacity in the feline lumbar spinal cord." J Neurosci **22**(8): 3130-3143.

Tillakaratne, N. J., M. Mouria, et al. (2000). "Increased expression of glutamate decarboxylase (GAD(67)) in feline lumbar spinal cord after complete thoracic spinal cord transection." J Neurosci Res **60**(2): 219-230.

Tokumoto, Y., S. Ogawa, et al. (2010). "Comparison of efficiency of terminal differentiation of oligodendrocytes from induced pluripotent stem cells versus embryonic stem cells in vitro." J Biosci Bioeng **109**(6): 622-628.

Tsuji, O., K. Miura, et al. (2010). "Therapeutic potential of appropriately evaluated safe-induced pluripotent stem cells for spinal cord injury." Proc Natl Acad Sci U S A **107**(28): 12704-12709.

Ullian, E. M., S. K. Sapperstein, et al. (2001). "Control of synapse number by glia." Science **291**(5504): 657-661.

Vaccarino, F. M., D. M. Fagel, et al. (2007). "Astroglial cells in development, regeneration, and repair." Neuroscientist **13**(2): 173-185.

Waters, R. L., I. H. Sie, et al. (1996). "Functional hand surgery following tetraplegia." Arch Phys Med Rehabil **77**(1): 86-94.

Weible, M. W., 2nd and T. Chan-Ling (2007). "Phenotypic characterization of neural stem cells from human fetal spinal cord: synergistic effect of LIF and BMP4 to generate astrocytes." Glia **55**(11): 1156-1168.

Wernig, M., J. P. Zhao, et al. (2008). "Neurons derived from reprogrammed fibroblasts functionally integrate into the fetal brain and improve symptoms of rats with Parkinson's disease." Proc Natl Acad Sci U S A **105**(15): 5856-5861.

Whishaw, I. Q. and S. M. Pellis (1990). "The structure of skilled forelimb reaching in the rat: a proximally driven movement with a single distal rotatory component." Behav Brain Res **41**(1): 49-59.

Wuolle, K. S., A. M. Bryden, et al. (2003). "Satisfaction with upper-extremity surgery in individuals with tetraplegia." Arch Phys Med Rehabil **84**(8): 1145-1149.

Yanagisawa, M., K. Nakashima, et al. (2001). "Signaling crosstalk underlying synergistic induction of astrocyte differentiation by BMPs and IL-6 family of cytokines." FEBS Lett **489**(2-3): 139-143.

Yang, Y., S. Vidensky, et al. (2011). "Molecular comparison of GLT1+ and ALDH1L1+ astrocytes in vivo in astroglial reporter mice." Glia **59**(2): 200-207.

Yeh, T. H., Y. Lee da, et al. (2009). "Microarray analyses reveal regional astrocyte heterogeneity with implications for neurofibromatosis type 1 (NF1)-regulated glial proliferation." Glia **57**(11): 1239-1249.

Yu, J., M. A. Vodyanik, et al. (2007). "Induced pluripotent stem cell lines derived from human somatic cells." Science **318**(5858): 1917-1920.

Yuan, S. H., J. Martin, et al. (2011). "Cell-surface marker signatures for the isolation of neural stem cells, glia and neurons derived from human pluripotent stem cells." PLoS One **6**(3): e17540.

Zhang, J. and L. Li (2005). "BMP signaling and stem cell regulation." Dev Biol **284**(1): 1-11.

Zhang, S. C., M. Wernig, et al. (2001). "In vitro differentiation of transplantable neural precursors from human embryonic stem cells." Nat Biotechnol **19**(12): 1129-1133.

Zhang, Y. and B. A. Barres (2010). "Astrocyte heterogeneity: an underappreciated topic in neurobiology." Curr Opin Neurobiol **20**(5): 588-594.

Zhao, R. and G. Q. Daley (2008). "From fibroblasts to iPS cells: induced pluripotency by defined factors." J Cell Biochem **105**(4): 949-955.

VITA

Samuel Nutt was born in Charlottesville, VA. He has lived in many places being the son of two dangerously overeducated parents who pursued their various degrees all over the country. At the University of Southern California he earned a Bachelor of Science degree in Biomedical Engineering. In 2003 he enrolled in the University of Washington's Medical Scientist Training Program and earned a Doctor of Philosophy in Neurobiology & Behavior, and expects to receive his Doctor of Medicine in 2014.